Lawrence Berkeley National Laboratory
Recent Work

Title
SPALLATION FISSION COMPETITION FROM THE COMPOUND SYSTEM U233 PLUS He4

Permalink
https://escholarship.org/uc/item/4ff7s2qx

Author
Thomas, Thomas D.

Publication Date
1957-07-01

eScholarship.org Powered by the California Digital Library
University of California

UCRL 3791
C.2

UNIVERSITY OF CALIFORNIA

Radiation Laboratory

TWO-WEEK LOAN COPY

This is a Library Circulating Copy which may be borrowed for two weeks. For a personal retention copy, call Tech. Info. Division, Ext. 5545

SPALLATION-FISSION COMPETITION FROM THE COMPOUND SYSTEM U^{233} PLUS He^{4}

BERKELEY, CALIFORNIA

DISCLAIMER

This document was prepared as an account of work sponsored by the United States Government. While this document is believed to contain correct information, neither the United States Government nor any agency thereof, nor the Regents of the University of California, nor any of their employees, makes any warranty, express or implied, or assumes any legal responsibility for the accuracy, completeness, or usefulness of any information, apparatus, product, or process disclosed, or represents that its use would not infringe privately owned rights. Reference herein to any specific commercial product, process, or service by its trade name, trademark, manufacturer, or otherwise, does not necessarily constitute or imply its endorsement, recommendation, or favoring by the United States Government or any agency thereof, or the Regents of the University of California. The views and opinions of authors expressed herein do not necessarily state or reflect those of the United States Government or any agency thereof or the Regents of the University of California.

UCRL-3791

UNIVERSITY OF CALIFORNIA

Radiation Laboratory
Berkeley, California

Contract No. W-7405-eng-48

SPALLATION-FISSION COMPETITION FROM THE COMPOUND SYSTEM U^{233} PLUS He^{4}

Thomas Darrah Thomas

(Thesis)

July, 1957

Printed for the U. S. Atomic Energy Commission

"So the atoms in turn, we now clearly discern,
Fly to bits with the utmost facility;
They wend on their way, and, in splitting, display
An absolute lack of stability."

Sir Wm. Ramsay, Ind. Eng. Chem.,
News Ed., 8, 18 (1930).

SPALLATION-FISSION COMPETITION FROM THE COMPOUND SYSTEM U^{233} PLUS He^{4}

Contents

SPALLATION-FISSION COMPETITION FROM THE COMPOUND SYSTEM U^{233} PLUS He^4

T. Darrah Thomas

Radiation Laboratory
University of California
Berkeley, California

July, 1957

ABSTRACT

The results of a series of experiments to study the competition between spallation and fission in the reactions induced in U^{233} with helium ions of energies between 20 and 46 Mev are given. The striking features of the excitation functions are the lowness of the (α,xn) cross sections compared with cross sections for the same reactions in other very heavy elements and the prominence of the (α,pxn) reactions.

The results are interpreted in terms of reaction mechanisms involving either the formation of a compound nucleus or direct interactions between the projectile and the nucleons in the surface of the nucleus. Fission competes more successfully against the compound nucleus spallation reactions in the reactions of U^{233} than in those of other very heavy elements; in general, the products of the direct interaction reactions are able to survive fission equally well for all targets.

A partial explanation for the relative fissionability of U^{233} and Pu^{239} is given in terms of the neutron binding energies of the products. A model for the compound nucleus reactions, based on a model by Jackson, is presented and it is shown that cross sections calculated on the basis of this model are in approximate agreement with the experimental values. Possible mechanisms for the direct interaction reactions are discussed.

The identification and decay properties of the new isotope, Pu^{233}, are described.

I. INTRODUCTION

The existence of the fission process among the nuclear reactions of the heavy elements makes the study of these reactions doubly interesting. First, fission (which does not occur abundantly in light elements except at very high excitations) is interesting in its own right. Second, competition between fission and nonfission, or spallation, reactions makes it possible to draw conclusions as to the mechanisms of the spallation reactions. It has been fruitful to study reactions induced by charged particles of energies less than 50 Mev, partly because of the availability of a fairly intense source of such particles in the Crocker Laboratory 60-inch cyclotron, but chiefly because it is possible to make a qualitative interpretation of the results in terms of the relatively simple compound-nucleus theory, without having to be concerned with such effects as nuclear transparency. The work presented here is a study of the spallation and fission reactions induced in uranium-233 by helium nuclei of energies from 20 to 46 Mev.

The Compound Nucleus

The compound-nucleus theory, first put forth by Bohr,[1] states that the nuclear reaction

$$A + a \longrightarrow B + b$$

(where A and B are the target and residual nuclei, respectively, and a and b are the projectile and emitted particle(s), respectively) proceeds through an intermediate state, or "compound nucleus",

$$A + a \longrightarrow C \longrightarrow B + b.$$

The lifetime of C is long enough that the energy of the incoming particle a is distributed throughout the nucleons of C and the nucleus "forgets" its mode of formation. However, invariants such as energy, momentum, angular momentum, and (probably) parity must be conserved. Thus, two compound nuclei, C and C', formed by two different reactions,

$$A + a \longrightarrow C$$

$$\text{and } D + d \longrightarrow C'$$

and having the same Z, A, energy, angular momentum, and parity, are indistinguishable.

The decay of the compound nucleus to products B and b can be described in terms similar to those used to describe ordinary nuclear disintegrations. The compound nucleus C is said to have a level width Γ if the reciprocal mean lifetime of the nucleus is $\Gamma/\hbar$. Γ thus has the dimensions of energy. If the nucleus can decay by several independent paths, we have

$$\Gamma_{\text{total}} = \sum_i \Gamma_i ,$$

where the summation is made over the various modes of decay. The cross section σ_i for a particular reaction is given by the expression

$$\sigma_i = \sigma_c \frac{\Gamma_i}{\Gamma_{\text{total}}} ,$$

where σ_c is the cross section for the formation of the compound nucleus.

Fission

It has been hoped that the study of spallation-fission competition would lead to a clearer understanding of the rather puzzling process of fission. Shortly after its discovery in 1939 by Hahn and Strassman,[2] fission was described by Bohr and Wheeler[3] and by Frenkel[4] in terms of the liquid-drop or compound-nucleus, model. On the basis of the liquid-drop model, Bohr and Wheeler predicted that fissionability should depend on Z^2/A. It was later demonstrated independently by Seaborg[5] and by Whitehouse and Galbraith[6] that spontaneous fission rates showed a direct dependence on Z^2/A of the fissioning nucleus. However, the dependence on Z^2/A is only approximate. Swiatecki,[7] by correcting the fission rates for irregularities in the mass surface, has been able to show a linear dependence of the logarithim of the spontaneous fission half life with Z^2/A. Vandenbosch[8] has found a correlation between the cross section for the $(\alpha,4n)$ reaction in heavy elements (a sensitive measure of fissionability) and Z^2/A.

It is in the mass distribution of the fission products that fission has been least understood. It has been found that for excitation energies of 10 to 20 Mev or less the nucleus of a very heavy element preferentially forms a heavy fragment of mass about 140 and a light fragment of mass 100 when it fissions.[9] This phenomenon is known as asymmetric fission. A

plot of yield of fission products versus mass number shows two peaks with a valley in between, meaning that at low excitations symmetric fission is unlikely -- just the opposite of what was predicted on the basis of the liquid-drop model.[10,11] As the excitation energy of the fissioning nucleus is increased, the valley rises rapidly and, at high excitations, fission becomes predominantly symmetric.[9]

A number of explanations of asymmetric fission have been advanced. Mayer,[12] Meitner,[13] and Curie[14] have suggested that the asymmetry is due to a tendency of the nucleus to fission to a pair of fragments, one of which has a "magic number" of neutrons and protons. Hill and Wheeler[11] have proposed an explanation that as the nucleus is deformed the even-parity levels are pushed to higher energies, with the result that further deformation is possible only if the nucleus can slip from the even-parity levels to the lower-energy odd-parity levels. According to Hill and Wheeler, such slippage is possible only if the nucleus is asymmetrically deformed. Frenkel[15] has suggested that, because of its lower reduced mass, a nucleus in an asymmetric deformation can penetrate the fission barrier more readily than can one in a symmetric deformation.

Fong[16] has given an explanation for asymmetric fission in terms of the masses of the fission fragments. Because of shell effects, the masses of the asymmetric fragments will be lower than those of the symmetric fragments. The result is that the asymmetric fragments will have a higher excitation energy and, hence, a higher level density than the symmetric. If, as Fong assumes, fission is a slow enough process that equilibrium is established among the various possible states at every moment during fission, there will be more nuclei passing through the configurations having high level densities at the instant of separation i.e., the asymmetric configurations.

The unified model of Bohr and Mottelson[17,18] provides still another explanation of asymmetric fission. As the excited nucleus approaches the saddle point (the highest energy point along the most energetically favorable reaction path leading to fission), its excitation energy is converted into potential energy of deformation, with

the result that at the saddle point the nucleus is "cold". Only a few, widely spaced levels will be available to the nucleus, and the spins and parities of these levels will probably have a marked effect on the mode of fission. It is thought that the spectrum of low-lying levels at the saddle point will resemble that of the levels of the nucleus near its ground state configuration. The existence of low-lying odd-parity states in even-even nuclei of the heavy elements can be explained by assuming that the nucleus is "pear shaped". If the spectrum of levels at the saddle point is to be similar to that near the ground state configuration, the nucleus will probably also have a pear-shaped, or asymmetric, mass distribution as it passes over the saddle point. At higher excitation energies, levels that do not involve an asymmetric shape for the nucleus will become available, and fission will become more symmetric.

Previous Work on Spallation-Fission Competition

The initial studies of spallation-fission competition in the very heavy elements were done by Glass, Carr, Cobble, and Seaborg,[19] who studied the reactions induced in Pu^{238}, Pu^{239}, and Pu^{242} by helium nuclei. This study has been extended to reactions induced in uranium isotopes with helium nuclei by Ritsema,[20] Vandenbosch,[21] Gordon,[22] Donovan,[23] and this author; in Np^{237} with helium ions by Gibson;[25] in Th^{232} with helium ions by Foreman;[26] and in plutonium, neptunium, and uranium isotopes with deuterons by Gibson,[25] Luoma,[27] Vandenbosch,[21] and Lessler.[28] Less detailed studies have been made among the heavier actinide elements by Harvey, Chetham-Strode, Ghiorso, Choppin, and Thompson.[29]

Glass, Carr, Cobble, and Seaborg[19] observed that the greatest part of the reaction cross section was taken up by fission, with the result that the fission cross section is not a sensitive measurement of the relative fissionability of different compound nuclei. Since $\sigma_{fission}$ is approximately equal to σ_c, it follows that Γ_{total} is approximately equal to $\Gamma_{fission}$ and, hence,

$$\sigma_{spallation} \approx \sigma_c \frac{\Gamma_{spallation}}{\Gamma_{fission}}.$$

Therefore, an increase in the half width of a nucleus for fission will result in a corresponding decrease in the cross section for spallation. The result is that it is possible to compare the relative fissionability of two nuclei by comparing the cross sections of these nuclei to undergo spallation reactions that proceed by way of a compound nucleus. Glass and co-workers observed a marked increase in the $(\alpha,2n)$ and $(\alpha,4n)$ cross sections in going from Pu^{238} to Pu^{242}. Since the greater part of these reactions probably takes place by the formation of a compound nucleus, they concluded that fission was competing with spallation more successfully in the reactions of the light plutonium isotopes than in those of the heavy plutonium isotopes.

On the other hand, Glass and co-workers found that reactions involving the emission of charged particles were able to compete fairly successfully against fission. Often cross sections for the emission of charged particles were equal to or greater than those for the emission of an equal number of neutrons. This phenomenon is particularly surprising in view of the fact that among the reactions of lighter elements, where the competition from fission is negligible, the cross sections for charged-particle emission at these energies are an order of magnitude lower than those for neutron emission.[30] The conclusion is that reactions involving charged-particle emission do not proceed by the formation of a compound nucleus, but rather by some direct interaction between the projectile and the target nucleus, probably with the emission of a complex charged particle such as a deuteron or a triton. This explanation has been borne out by the work of Wade, Gonzalez-Vidal, Glass, and Seaborg,[31] who have measured directly the amount of tritium produced when various elements are bombarded with helium nuclei, deuterons, and protons.

It was found by Glass and co-workers that the valley in the curve of the fission mass yield rose rapidly with increased energy of bombarding particle (and, hence, increasing excitation energy of the compound nucleus), and that fission induced by helium nuclei of 30 to 45 Mev was predominantly symmetric.

Previous studies of the charged-particle-induced spallation reactions of U^{233} have been done by Hyde, Studier, and Ghiorso,[32] who produced

the nuclides Np^{234}, Np^{235}, and Pu^{234}; Perlman, Morgan, and O'Connor,[33] who produced Np^{234}, Pu^{234}, and Pu^{236} and measured cross sections for their production with 44-Mev helium ions; Magnusson, Thompson, and Seaborg,[34] who produced Np^{231}, Np^{232} and Np^{233}; and Orth,[35] who produced Np^{234}, Pu^{232}, Pu^{234}, and Pu^{235}. The cross sections measured by Perlman, Morgan, and O'Connor[33] of 0.5 mb for the (α,n) reaction and 1 mb for the $(\alpha,3n)$ reaction at 44 Mev are in good agreement with those determined in this work; their cross section of 0.2 mb for the $(\alpha,p2n)$ reaction is low by two orders of magnitude. Gibson[25] has studied the competition between spallation and fission induced in U^{233} by deuterons, and Cohen, Ferrell-Bryan, Coombes, and Hullings[36] have measured the angular distribution of the fission fragments from fission induced by 22-Mev protons. (No attempt will be made to review the work done on the reactions induced in U^{233} by neutrons and photons.)

This Work

The work to be described here is part of a program to determine to what extent the pronounced mass effect on spallation-fission competition that was observed in the reactions of the plutonium isotopes will also appear in those of the uranium isotopes; to study the effect of varying the charge of the target nucleus; and to look for possible effects of odd nucleons. The comparison of the reactions of U^{233} with those of Pu^{239} [19] should be particularly fruitful, since the two are analagous nuclei, differing in mass and charge by two protons and four neutrons and each being the first beta-stable odd-mass isotope of its element. Comparison of these results with those of Gordon[22] and Ritsema[20] on U^{234} and U^{238} should reveal any odd-even effect, and with those of Vandenbosch[21] on U^{235} any mass effect.

II. EXPERIMENTAL WORK

Target Material

The U^{233} used in these bombardments was obtained from various sources. One sample was subjected to mass analysis and found to contain about 3% U^{238} and less than 1% U^{234} and U^{235}. For purposes of calculating cross sections, it was assumed that the material was 100% U^{233}. A pulse analysis of the alpha particles emitted from the U^{233} showed that about 1% of the activity was due to U^{232}. The contribution of the U^{232} was neglected in the calculations. Because of the high specific activity of U^{233}, all operations involving the handling of more than 100 μg of the isotope were carried out in a "glove box".[37]

A number of purification procedures were used on the target material at various stages during the course of these experiments. The four most common were extraction of the uranium into ethyl ether (a procedure that proved to be unfailingly unsuccessful), extraction into a solution of tributylphosphate in carbon tetrachloride, precipitation of uranyl hydroxide and ferric hydroxide followed by the dissolving of the uranium in a solution of sodium carbonate, and adsorption of the uranium from concentrated hydrochloric acid onto an ion-exchange column packed with Dowex A-1 anion-exchange resin followed by an elution with hydrochloric acid of concentration between 0.1 and 1 M. For purifying the uranium from large amounts of aluminum, iron, and fission products, the tributyl phosphate extraction was found to be the most reliable method. The hydroxide-carbonate cycle worked well for large amounts of uranium (except for an occasional disaster due to overexuberant effervescence). The anion-exchange procedure was used as a final purification step, but was not a useful method of freeing the uranium from iron.

Target Preparation

The U^{233} was electrodeposited as a hydrated oxide on dish-shaped pieces of aluminum (hereinafter referred to as "hats"), 10 mil thick and about 7/8 inch in diameter. The plating procedure was been described by Hufford and Scott.[38] The amount of uranium that had been plated was

determined from the specific activity of U^{233} (2.10×10^7 d/m per mg) and the disintegration rate of the sample measured in one of two alpha-particle counters of known geometry. In some cases the activity was measured in both counters with agreement to a few percent.

It was necessary to know whether or not the uranium was evenly deposited over the surface of the hat. To determine the uniformity of the target, I masked the target with an aluminum disk from which a small hole or a quadrant had been cut, and measured the activity coming from the unmasked area. A comparison of several such measurements, each with a different part of the target covered, showed whether or not the target was uniform. In general, four such determinations were within 10% of their average, although some targets were used in which the agreement was no better than 20%.

The area of the target was determined by measuring the diameter of the target. This measurement is perhaps one of the largest sources of error, because the targets were not perfectly circular and the measured diameter is only an average of several measurements, and because a 3% to 5% error in measuring the diameter becomes a 6% to 10% error in the area.

For the bombardments, the targets were mounted in one of two assemblies. In the first ten bombardments, a "pistol grip" target holder, described by Glass,[39] was used. For all later bombardments, a micro-target assembly described by Ritsema[20] was used. The target was always covered by a 1-mil aluminum foil, which caught the reaction products that recoiled from the target in the forward direction.

The Beam of Helium Ions

The helium ions emerging from the Crocker Laboratory 60-inch cyclotron have a range in aluminum of 231 mg/cm^2 with a variation of perhaps 5 mg/cm^2. According to the range-energy curves of Aron, Hoffman, and Williams,[40] a range of 231 mg/cm^2 corresponds to an energy of 48.3 Mev. Aluminum and platinum foils were placed between the emergent beam and the target to lower the energy to any desired bombarding energy. Again the curves of Aron, Hoffman, and Williams[40] were used for aluminum, and a curve interpolated between two of their curves was used for platinum, to determine the bombarding energy.

At full energy the cyclotron beam was an energy spread of about 2%, or 1 Mev. The effect of passing the beam through degrading foils is to increase the energy spread, with the result that the spread at 20 Mev is somewhat greater than 1 Mev. This spread causes a significant error in measured cross sections only if the energy is such that the excitation function is either rising or falling sharply, since under these conditions a small contribution from the high- or low-energy portion of the beam would cause the cross section at a given energy to appear to be higher than it actually is.

During the bombardments, the target holder was insulated from the cyclotron and from ground, so that it was possible to measure the beam intensity from the rate of accumulation of charge on the target holder. In general, the beam intensity was recorded by a Speedomax recorder, and invariably the total integrated beam was recorded. The beam-monitoring device was calibrated frequently so that the beam intensity was known to an accuracy of 0.5%.

Since it was important that all the beam measured should strike the target within the uniformly plated area, the beam was collimated with a 5/8-inch collimator. Before most of the bombardments in which the pistol-grip target holder was used, a piece of Scotch tape was placed over the target and bombarded for a few seconds. From the pattern of the burned area on the Scotch tape it was possible to tell whether or not the target was well centered with respect to the beam. For those bombardments in which the microtarget assembly was used it was impractical to measure a beam pattern. However, it was possible to tell from examination of the aluminum target hat after the bombardment whether or not all of the beam had struck the target. A beam pattern showed either on the back of the hat, or on the front just after the uranium had been dissolved.

Chemical Procedures

The chemical procedures that were used in this work have many origins, and it is nearly impossible to give any one person credit for a particular procedure. Two procedures were used for the separation of neptunium and plutonium. The first, which was devised by the author,

proved to be too slow, to give an insufficient purification, and to give too low a yield of neptunium. The second was a modification of one devised by Magnusson, Huizenga, Siddall, and Studier.[41] Many of the procedures for the separation of the fission products are from the compilations by Meinke[42] and Lindner.[43]

Dissolution of the Target

The target, aluminum hat, and cover foil were dissolved in aqua regia containing known amounts of Np^{237} and Pu^{239} tracers and fission product carriers from which the chemical yields of the various products were to be determined.

Separation of Neptunium and Plutonium

In the first procedure mentioned above, cerium, which had been added as a carrier, was precipitated as cerous hydroxide by the addition of sodium hydroxide. The aluminum stayed in solution as aluminate ion, while neptunium, plutonium, the lanthanides, zirconium, and other fission products coprecipitated with the cerous hydroxide. The hydroxide precipitate was redissolved in hydrochloric acid, and hydrofluoric acid was added to precipitate cerous fluoride. Only the actinides and lanthanides coprecipitated with the fluoride. The cerous fluoride was dissolved in a solution of 6 M nitric acid saturated with boric acid, and cerous hydroxide (carrying with it the actinides and lanthanides) was precipitated with ammonium hydroxide. The hydroxide precipitate was redissolved in concentrated hydrochloric acid and the solution passed through an ion-exchange column (3mm by 2 cm) packed with Dowex A-1 anion exchange resin. The actinides in oxidation states greater than +3 adsorb strongly on such a column from concentrated hydrochloric acid, whereas the lanthanides wash through. The column was washed with additional concentrated hydrochloric acid to ensure the removal of the lanthanides. The actinides were stripped from the column with 1 M hydrochloric acid into a solution containing enough hydrochloric acid, hydriodic acid, and hydrazine dihydrochloride so that the resulting solution was 1 M in hydrochloric acid, 0.1 M in hydriodic acid, and 0.005 M in hydrazine. The solution was heated to reduce the plutonium to the (III) state and neptunium to

the (IV) state, cooled, saturated with hydrogen chloride gas, and passed through a second ion-enchange column similar to the first. Under these conditions the neptunium (IV) is adsorbed, while the plutonium (III) washes through. When the column had been washed with additional concentrated hydrochloric acid made 0.1 M in hydriodic acid, the neptunium was stripped with 1 M hydrochloric acid and further purified by an extraction into a benzene solution of thenoyltrifluoroacetone (TTA), a procedure which is described below. The neptunium and plutonium were then mounted on platinum disks for counting (see below).

In the second procedure, after the dissolution of the target, ferrous ion and hydrazine dihydrochloride were added to the solution to make the final concentration 0.005 M in ferrous ion and 0.1 M in hydrazine. The solution was heated in a hot water bath at 90° C for 5 minutes to reduce neptunium to the (IV) state and plutonium to the (III) state. Addition of enough orthophosphoric acid to make the solution 0.5 M in phosphoric acid precipitated the zirconium fission-product carrier as the phosphate. The neptunium (IV) coprecipitated with the zirconium phosphate.* In some of the later bombardments, 200 micrograms of Th^{232} were added and a second zirconium phosphate precipitation was made to ensure removal of the Th^{228} daughter of U^{232} from the plutonium. Because the products of the $(\alpha,2n)$, $(\alpha,4n)$, and $(\alpha,5n)$ reactions, Pu^{235}, Pu^{233}, and Pu^{232}, have short half lives, the precipitate containing the neptunium and zirconium was set aside at this point and the purification of the plutonium was continued. The plutonium was oxidized to the (IV) state by making the solution 0.1 M in sodium bromate and heating in the water bath for 1 minute.

---

*The first zirconium phosphate precipitate did not always form readily, and a heating period of several minutes was sometimes necessary to coagulate the precipitate. A possible explanation of this phenomenon is that the zirconium forms a stable complex with chloride, with the result that the rate of formation of zirconium phosphate is slow. It should be noted that when second and third zirconium phosphate precipitations were made the precipitates formed readily.

About 10 mg of zirconium was added; the plutonium (IV) coprecipitated with the resulting zirconium phosphate precipitate. The precipitate was washed with a solution 0.5 M in nitric acid and 0.05 M in orthophosphoric acid and dissolved in a solution 1 M in nitric acid and 1 M in hydrofluoric acid. The addition of 2 mg of lanthanum precipitated lanthanum fluoride, with which the plutonium coprecipitated. The fluoride was redissolved in 6 M nitric acid saturated with boric acid, and ammonium hydroxide was added to the resulting solution to precipitate lanthanum hydroxide. The hydroxide was dissolved in concentrated hydrochloric acid, and the solution was passed through a short column (3mm by 1 cm) of Dowex A-1 anion-exchange resin. When the column had been washed with concentrated hydrochloric acid to remove any traces of lanthanum, a solution of concentrated hydrochloric acid made 0.1 M in hydriodic acid was passed through the column at the rate of two drops a minute. The hydriodic acid reduced the plutonium to the (III) state, which is not adsorbed on the resin. About 14 drops were necessary to remove most of the plutonium from the column. The plutonium was then mounted on platinum (see below). The chemical yield of plutonium ranged from 10% to 40%.

The neptunium separation procedure is identical to the plutonium procedure from the precipitation of the zirconium phosphate to the precipitation of the lanthanum hydroxide, with the exception that small amounts of ferrous ion and hydrazine were added to the solution with which the zirconium phosphate was washed. This technique helped to remove any plutonium that had not been reduced initially, and the washings were therefore added to the solution from which the plutonium was to be removed. The lanthanum hydroxide was dissolved in 4 milliequivalents of concentrated hydrochloric acid, and the solution diluted to 2.0 ml. Four-tenths ml of 1 M hydroxylamine was added and the solution heated for 1 minute to reduce any plutonium that might still have been present. Two drops of 1 M stannous chloride and 1.6 ml of 2.5 M potassium iodide were added, and the solution was heated in boiling water for 10 minutes. Any neptunium that might have been oxidized during the earlier steps was reduced to the (IV) state by this step. The solution was cooled and

stirred vigorously with 2 ml of a 0.4 M solution of thenoyltrifluoroacetone for 20 minutes (5 minutes when the short-lived isotope Np^{233} was thought to be present). The organic phase was washed twice with 2-ml portions of 1 M hydrochloric acid for 3 minutes each, and the neptunium was back-extracted into 8 M hydrochloric acid for 20 minutes (5 minutes when Np^{233} was present). The reason for the back-extraction is that any zirconium that may have followed the neptunium through the thenoyltrifluoroacetone extraction does not back-extract into 8 M hydrochloric acid. The acid was washed with an equal volume of benzene for 3 minutes to remove any thenoltrifluoroacetone and the sample was mounted on platinum. The chemical yield of neptunium ranged from 1% to 30%.[44]

Fission-Product Procedures

When the first procedure for the separation of neptunium and plutonium was used, the only fission products taken out were zirconium, cadmium, cerium, and -- on a few bombardments -- other lanthanides. The zirconium precipitated as a hydroxide with the cerous hydroxide, but remained in the supernatant solution when cerous fluoride was precipitated. Barium chloride was added to this solution to precipitate barium fluozirconate, and the zirconium was purified by a procedure devised by Iddings and described by Lindner,[43] involving an extraction with thenoyltrifluoroacetone.

Cadmium hydroxide, which precipitated slowly from the solution left after the cerous hydroxide had been precipitated, was dissolved in hydrochloric acid. (Since cadmium forms a chloride complex which hinders the formation of a sulfide precipitate, the hydroxide should have been dissolved in sulfuric acid.) The acid was diluted to about 0.5 M, and hydrogen sulfide gas was bubbled into the solution to precipitate cadmium sulfide. The sulfide was dissolved in hydrochloric acid and passed through an ion-exchange column (5mm by 5 cm) packed with Dowex A-1 anion-exchange resin, which adsorbs cadmium from hydrochloric acid. The column was washed with 1 M hydrochloric acid, and the cadmium removed with 0.75 M sulfuric acid. The column effluent was diluted to 0.5 M

acid and saturated with hydrogen sulfide gas. The resulting sulfide precipitate was dissolved in 4 M hydrochloric acid, antimony (III) carrier was added as a scavenger, and the solution was saturated with hydrogen sulfide to precipitate antimonous sulfide. When the supernatant solution was diluted to an acid concentration of less than 0.5 M, cadmium sulfide precipitated.

The cerium and the rare earth fraction was found in the effluent from the first anion-exchange column. When cerium was the only lanthanide to be isolated, an oxidation-reduction cycle developed by Hicks and described by Lindner[43] was used as the purification procedure. When other rare earths were to be separated, an ion-exchange column packed with Dowex-50 cation-exchange resin was used. Hydrofluoric acid was added to the effluent from the anion-exchange column to precipitate the rare earth fluorides. This precipitate was dissolved in 6 M nitric acid saturated with boric acid. Ammonium hydroxide was added to precipitate the rare earth hydroxides, which were redissolved in 2 M hydrochloric acid and adsorbed onto 1 ml of Dowex-50 resin. The resin was placed on the top of the column and the rare earths eluted with a mixture of lactic acid and ammonium lactate with a pH varying continuously from about 3 to about 5, according to the procedure described by Nervik.[45]

When the second neptunium and plutonium separation procedure was used, fission-product carriers were added for strontium, zirconium, cadmium, and barium. On a few bombardments ruthenium and lanthanides were also added.

Ruthenium was reduced to the metal when the target hat was dissolved and was removed by centrifugation. The metal was dissolved in a mixture of nitric and hydrochloric acids and added to a mixture of sodium bismuthate, perchloric acid, orthophosphoric acid, and sodium iodide, from which ruthenium tetroxide was distilled. The distillate was absorbed in 6 M sodium hydroxide, to which ethanol was added to precipitate ruthenium dioxide. The dioxide was dissolved in hydrochloric acid, and the ruthenium was reduced to the metal with magnesium powder. The cross sections that were based on ruthenium activity purified by this method were uniformly low, both in this work and in

the work of Vandenbosch,[21] relative to those for other elements of approximately the same mass number. It is thought that the rate of isotopic exchange among the various oxidation states of ruthenium is slow, with the result that the measured chemical yield of carrier does not represent the true yield of radioactive material. On three bombardments, aliquots of the target solution were added to ruthenium carrier, which was then distilled directly, without precipitation of the metal until the final step. Results obtained by this method were higher in both the U^{233} and the U^{235} work than those obtained by the method involving the initial precipitation of the metal.

To the supernatant solution from the final zirconium phosphate precipitation were added sodium hydroxide and sodium carbonate to precipitate barium, strontium, some cadmium, and the lanthanides. The precipitate was dissolved in hydrochloric acid and the solution, cooled in an ice bath, was saturated with hydrogen chloride gas to precipitate barium and strontium chlorides. The supernatant solution from the hydroxide-carbonate precipitation was saturated with hydrogen sulfide gas to precipitate cadmium and ferrous sulfides, which were dissolved in concentrated hydrochloric acid and added to the solution remaining after the precipitation of the alkaline earth chlorides. The chloride solution was passed through an ion-exchange column (5mm by 5 cm) packed with Dowex A-1 anion-exchange resin. The lanthanides passed through and were purified as described above; iron and cadmium were adsorbed. The iron was removed by washing the column with 1 M hydrochloric acid, and the cadmium by washing with 0.75 M sulfuric acid. The cadmium was then treated as before.

The barium and strontium chlorides were dissolved in water and reprecipitated with hydrogen chloride gas. The precipitates were again dissolved in water, the pH of the solution was adjusted to 5 with a sodium acetate–acetic acid buffer, and barium chromate was precipitated. The barium chromate was metathesized to barium carbonate with hot 6 M sodium carbonate. The carbonate was redissolved in nitric acid, and a few milligrams of strontium holdback carrier was added. The pH of the solution was again buffered to 5, and barium carbonate reprecipitated.

The supernatant solution from the first barium chromate precipitation was made basic with ammonium hydroxide, and sodium carbonate was added to precipitate strontium carbonate. The precipitate was dissolved in nitric acid, and barium holdback carrier added. Barium chromate and strontium carbonate were then precipitated as before and the barium discarded.

The zirconium, which had been precipitated as zirconium phosphate in the neptunium chemistry, remained in the supernatant solution when the lanthanum fluoride was precipitated. As before, barium chloride was added to precipitate barium fluozirconate, and the zirconium was purified by the procedure of Iddings mentioned above.[43]

In three bombardments, aliquots of the target solution were added to previously measured amounts of ruthenium, molybdenum, and silver carriers. One aliquot was used for both silver and molybdenum with the result that it was necessary to separate the silver from the molybdenum. Two methods were used. In the first, the silver was precipitated as silver chloride by dilution of the solution (enough hydrochloric acid had been added to complex all the silver). In the second, the solution containing the molybdenum and the silver chloride complex was passed through an ion-exchange column (6 mm by 10 cm) packed with Dowex A-1 anion-exchange resin. The column was washed with 0.1 M hydrochloric acid and the silver removed with 3 M ammonium hydroxide. The molybdenum was stripped from the column with 6 M sodium hydroxide and purified by a procedure of Stevenson, Hicks, and Levy, reported by Lindner.[43] A procedure from Meinke[42] was used to purify the silver.

Mounting of Samples

Spallation Products

Since the energies of the alpha particles emitted from the samples were to be measured in an alpha pulse-height analyzer, and since it was necessary to detect the low-energy Auger electrons emitted during the electron-capture process, it was necessary to have very thin samples. At the beginning of these experiments, neptunium and plutonium were vaporized from a 1- or 2-mil tantalum filament heated to red heat under vacuum

onto a 1-inch diameter disk of 2-mil platinum placed about a centimeter above the filament. The vaporization technique had the disadvantages that it sometimes required as long as half an hour to pump down the apparatus to a low enough vacuum, and that occasionally tantalum would be vaporized onto the platinum plate.

The vaporization procedure was replaced by an electrodeposition procedure developed by Harvey and co-workers[29] and described in detail by Chetham-Strode.[46] A solution 6 M in ammonium chloride containing the material to be deposited was adjusted to just the acid side of the methyl red end point. A current of about 2 amperes was passed through the solution for 2 minutes with a 2-mil platinum disc serving as cathode. On this plate a very thin deposit of the sample was formed.

In some of the earlier bombardments, samples of plutonium were merely evaporated onto platinum plates.

The platinum plates used were always heated to red heat in the flame of a microburner before being used, and, when either the electrodeposition or the evaporation technique was used, the plates were again so heated before the samples were placed in a counter. The purpose of the heating was to destroy any organic matter, which might cause thickness of the sample, and to make the material adhere more firmly to the plate.

Fission Products

The purified fission products were taken up in either acetone or ethanol and slurried onto previously weighed aluminum dishes 2 mils thick and 1-inch in diameter. The samples were dried under a heat lamp and weighed. A few drops of Zapon, a colorless lacquer, (Atlas Powder Co., North Chicago, Illinois) were placed on the sample to hold it to the dish and dried under a heat lamp. The dishes were mounted on rectangles of aluminum 2.5 by 3.5 inches and 50 mils thick.

Detection of Radiations

Spallation Products

All the spallation products produced in these bombardments decay by either electron capture or alpha emission, or both.[47] (Np^{236} decays by negative beta-particle emission as well as by electron capture, and Np^{234} is known to decay by positron emission,[48] although the predominant mode of decay is electron capture.)

Alpha particles were detected in an argon-flow windowless ionization chamber of 52% geometry, and in one of three alpha pulse-height analyzers. From the pulse analyses it was possible to determine what fraction of the alpha particles were due to the decay of a particular isotope, and from the counts taken at 52% geometry it was possible to determine the absolute disintegration rate of any alpha-emitting nuclide present.

A continuous-flow-methane windowless proportional counter, the Nucleometer (Radiation Counter Laboratories, Inc., Skokie, Illinois), was used to detect the Auger electrons accompanying electron capture. Unfortunately, the efficiency with which this instrument detects electron capture events varies from nuclide to nuclide, and probably depends on the decay scheme of the nuclide. It was therefore necessary to determine the counting efficiency, or ratio of number of events detected by the Nucleometer to number of disintegrations, for each nuclide studied. A discussion of methods of determining counting efficiencies and results of some determinations is found in Appendix A.

Fission Products

The radiations emitted from the fission products were counted in an end-window Geiger-Müller counter coupled to a standard scaling circuit. The tube on this counter was filled with a chlorine-argon mixture.

Treatment of Data

Decay Curves

Coincidence corrections were added to the observed counting rates and the resulting quantities were plotted on semilog graph paper as a function of time to give a "decay curve." Since, in general, several

nuclides decaying with different half lives were present in each sample, it was necessary to resolve the decay curves into their various components. Decay was followed until all but the last component had decayed away, i.e., until the decay curve was a straight line. This line was extrapolated back in time and its value was subtracted from that of the observed curve. The process was repeated until all the components had been resolved. However, it must be admitted that for curves having more than two components, the technique works better in theory than in practice. It was also sometimes necessary to correct for the increase in activity due to the growth of radioactive daughter nuclides. When the decay curves had been resolved, the activity of each component at the time of the end of the bombardment was calculated by extrapolating the various straight-line curves backward to the appropriate time.

Because the half lives of almost all the products were known it was possible and sometimes necessary to use such aids as the Biller[49] plot and the synthetic curves described by Shudde.[50] A new type of plot involving parent-and-daughter relationships was devised, and is described in Appendix B. An attempt was made to use the IBM 650 digital computer to make a least-squares fit to some of the decay curves, using Shudde's[50] method of fractional residuals. The results were satisfactory, but the method was time-consuming.

Corrections Applied to Alpha-Counting Data

Since most of the nuclides whose activities were determined by alpha-particle counting decayed also by electron capture, it was necessary to know the ratio of the number of disintegrations by alpha emission to the total number of disintegrations. The values of these ratios and their sources are given in Table I.

Table I. Percent alpha emission for plutonium isotopes

Nuclide	Percent alpha emission	Source
Pu^{236}	100.	a
Pu^{235}	0.003	b
Pu^{234}	5.46	c
Pu^{233}	0.12	d
Pu^{232}	11.2	e

a. See Reference 51.

b. This work. See Appendix A.

c. R. Hoff and F. Asaro, private communication.

d. This work. From estimated counting efficiency of daughter. See Chapter V.

e. Estimated from the alpha systematics. See Reference 51.

Corrections Applied to Geiger-Counter Counting Rates

Because of the physical arrangement of the Geiger counter and because of the nature of the interactions of beta particles with matter, it was necessary to make a number of corrections on the counting rates measured with the Geiger counter in order to obtain disintegration rates. The relation between disintegrations per minute, d/m, and counts per minute, c/m, is

$$d/m = c/m\ (f_{AW}) \ /\ (f_S f_{BS} f_G).$$

The various factors are discussed below.

The air-window correction, f_{AW}, is a correction for the fraction of the beta particles absorbed in the air between the sample and the counter and in the mica window of the counter. These factors were obtained from a curve of f_{AW} versus the maximum energy of the beta particle, based on the data of Ritsema.[20]

The self-scattering and self-absorption correction, f_S, is to correct for the beta particles which, originally moving away from the counter, are scattered by the sample back into the counter, and for the beta particles which are absorbed by the sample itself. These factors were obtained from the data of Nervik and Stevenson[52] for samples of lead nitrate and sodium chloride, using the interpolation formula

$$f_S = (f_S)_{Pb(NO_3)_2} - \left[(116 - Z)/116\right]\left[(f_S)_{Pb(NO_3)_2} - (f_S)_{NaCl}\right] ,$$

where Z is the sum of the charges of all the atoms represented by the formula for the compound being considered. There is no mathematical and practically no theoretical justification for this formula, but the factors determined from it are in fair agreement with the experimental values of Hicks and Gilbert.[53]

The backscattering correction, f_{BS}, is applied to correct for the beta particles scattered into the counter by the aluminum backing material. Enough aluminum was used so that the backing was in effect infinitely thick. The data of Burtt[54] was used to determine this factor.

The geometry factor, f_G, corrects for the fact that the Geiger counter does not subtend a solid angle of 4π steradians. Although it is possible to calculate the geometry correction factor, it was determined by measuring the counting rate of a Bureau of Standards sample of RaD of known disintegration rate. Correction was made on the counting rate of the standard for air-window absorption, self-scattering and self-absorption, and backscattering.

In the cases in which a nuclide decayed by emission of beta particles of several energies, and over-all correction factor was calculated from an approximate formula derived by Foreman and Glass[55]

$$\frac{f_{AW}}{f_S f_{BS} f_G} = \frac{1}{f_G \left(\Sigma_i x_i / f_{AW_i}\right)\left(\Sigma_i x_i f_{S_i} f_{BS_i}\right)} ,$$

where the summation is over the number of different-energy beta particles and x_i is the fraction of the total number of disintegrations that occur with emission of a beta particle with energy E_i. When there were

conversion electrons to be considered, it was assumed that a monoenergetic electron of energy E interacted with matter in the same manner as did a beta particle with a maximum energy $E_{max} = 3E$.

Calculation of Cross Sections

The cross section σ for a given reaction is given by the formula

$$\sigma = N/nIt,$$

where N is the number of atoms of product formed during the bombardment, n the number of target nuclei per square centimeter, and It the number of projectiles (current multiplied by time) striking the target. However, the quantity measured is disintegrations per minute at the end of the bombardment,

$$d/m = N(1 - e^{-\lambda t})/t,$$

where t is the length of the bombardment and λ is the decay constant of the product. Hence we have

$$\sigma = (d/m)/(1 - e^{-\lambda t})nI.$$

For the case in which the half life of the product is long compared with the bombardment time, we have

$$\sigma = (d/m)/\lambda nIt.$$

When a particular spallation product was also the daughter of a short-lived spallation product, the apparent cross section for the daughter was corrected by the formula

$$\sigma_d = \sigma_a - \sigma_p + \sigma_p \left[1 - (1 - e^{-\lambda_1 t_1})(e^{t_2(\lambda_2 - \lambda_1)})/(1 - e^{-\lambda_2 t_1}) \right],$$

where σ_d is the true cross section for production of the daughter, σ_a is the apparent cross section, σ_p the cross section for the production of the parent, λ_1 and λ_2 the decay constants of parent and daughter, respectively, t_1 the length of the bombardment, and t_2 the time between the end of the bombardment and the separation of the daughter from the parent. If the daughter has a long half life relative to t_1 and t_2, the formula simplifies to

$$\sigma_d = \sigma_a - \sigma_p + \sigma_p (1 - e^{-\lambda_1 t_1})(e^{-\lambda_1 t_2})/\lambda_1 t_1.$$

III. RESULTS

Spallation Cross Sections

The values for the cross sections for the (α,xn) and (α,pxn) reactions on U^{233}, together with the helium-ion energies at which these cross sections were observed are presented in Table II. The alpha branching ratios and counting efficiencies on which these values are based are listed in Table I (Chapter II) for the alpha branching ratios, and Table VI (Appendix A) for the counting efficiencies. In Figure 1 are plotted the cross sections for the (α,xn) reactions as a function of energy, with smooth curves drawn "through" the points. In Figure 2 are plotted the (α,pxn) cross sections. The (α,p) excitation functions represent a lower limit, since the yield of the long-lived isomer of Np^{236} was not measured.

Fission-Product Cross Sections

Mass Yields

The fissioning nucleus divides into two fragments such that the sum of the mass numbers of the two fragments plus the number of neutrons emitted equals the mass number of the fissioning nucleus and such that the sum of the charges of the two fragments equals the charge of the original nucleus. For a given mass distribution, more than one charge distribution is possible. It is reasonable to assume, however, that for a given mass distribution, there is a most probable charge distribution, and that the probability of finding other charge distributions decreases monotonically as one varies the charge distribution from the most probable one. Hence if, for a given set of isobars, we plot yield from fission of an isobar versus its atomic number, we will get a curve with a maximum. We will call the position of the maximum Z_p and note that Z_p is not necessarily an integer.

Ideally, in measuring the fission yield for a particular isobaric chain, we try to measure the yield of a nuclide whose $Z-Z_p$ is great enough that the nuclide is produced only by the negatron decay of other nuclides and not by direct fission. Hence, if the half lives of its radioactive precursors are short enough, the yield of this nuclide will

Table II

Cross sections for spallation reactions induced in U^{233} with helium ions

E (Mev)	Cross Section (millibarns)								
	(α,n)	(α,2n)	(α,3n)	(α,4n)	(α,5n)	(α,p)	(α,pn)	(α,p2n)	(α,p3n)
20.3	0.18								
23.5	0.42	1.30							
26.2	0.59	3.86	0.003			0.20	1.0	0.16	
28.9	0.96	6.54	0.094			0.53	-1.8	1.63	
29.4	0.64		0.066						
30.7						0.63	3.5	5.04	
31.8	1.01	3.40	1.03			1.72	0.3	4.91	
32.4			0.44			0.64		3.52	
34.3						1.07	13.5	10.9	
35.3	0.49	1.19	1.10			0.58	2.5	5.20	0.21
36.8						1.46	6.5	10.5	
36.8			0.76						
37.8	0.52	0.94	0.54			0.74	3.5	7.25	0.11
39.0			0.61						
40.0			0.50						
40.4						0.40	4.6	10.4	1.16
41.0	0.42	1.19	0.37			0.62	14.9	11.8	0.60
42.7			0.21	0.27	0.002	0.70	2.6	9.4	
43.8						2.53	8.8	17.8	1.41
44.3	0.73		0.29			0.72	18.7	19.9	1.72
44.4			0.57	1.03		0.66		15.9	0.64
46.2	0.79		0.51	1.13		0.30	21.3	19.6	1.10
46.2		1.31	0.23	0.33					
46.2			0.17	0.34					

be equal to the total fission yield for the isobaric chain. In practice, however, it is not always possible to pick such a nuclide, and it is often necessary to make a correction to the measured yield for those members of the chain having Z higher than the Z of the isolated nuclide.

It is possible to find some nuclides that, because of the existence of a long-lived isobar of lower Z, can be produced in measureable yield only by direct fission. If we measure the yields of a number of these shielded nuclides as well as the total yields of the isobaric chains, and if we have some way of determining Z_p, we may make a plot of the fraction of the chain yeild that is accounted for by the direct production of a nuclide with charge Z as a function of $Z-Z_p$, and thus obtain an empirical correction curve. Because the yields of nuclides from different regions of the periodic table, produced from fissioning nuclei of various excitation energies, are included in such a plot, the assumption must be made that the fractional yield is a function only of $Z-Z_p$ and is independent of the mass number of the isobaric chain and of the excitation energy of the fissioning nucleus. A further assumption has been made in this work that for fissioning nuclei in the range from Np^{235} to Am^{241} the fractional chain yield is independent of the fissioning nucleus.

The problem remains: what is the value of Z? One solution, due to Glendenin, Coryell, and Edwards, and developed by Pappas,[56] states that (Z_A-Z_p) of the light fragment is equal to (Z_A-Z_p) of the heavy fragment, where Z_A represents the charge of the most stable nuclide of mass A. Pappas has shown that, for low-energy fission, the data agree with his postulate.[56] A second solution, proposed by Goeckermann and Perlman, states that the two fragments have the same charge-to-mass ratio as the fissioning nucleus.[57] Gibson[25] has shown that, for moderate-energy fission, the data are in better agreement with the postulate of Goeckermann and Perlman than with that of Pappas.

In this work, four yields of shielded nuclides were measured -- three for Ba^{135m} and one for Pr^{142}. The yield of Ba^{135m} was multiplied by a factor of 4/3 to correct for the formation of the stable isomer, Ba^{135}, on the assumption that the ratio of the amount of Ba^{135m} formed to that of Ba^{135} would be given by

$$(2I + 1)_{135m}/(2I + 1)_{135},^{*}$$

which is equal to 3, where the I's represent the nuclear spins of the respective isomers. A first approximation to the total mass-135 yield was made on the basis of a curve of fission yield versus mass number drawn through the uncorrected points. No second approximation was made. For the Pr^{142}, it was assumed that the total mass-142 chain yield was approximately equal to the mass-143 chain yield, based on the yield of Pr^{143}, measured at the same time as that of Pr^{142}. The values of the fractional chain yield so determined together with one point measured by Vandenbosch[21] were plotted on the curves of Gibson. It was found that the points plotted against a $Z-Z_p$ calculated on the basis of the postulate of Goeckermann and Perlman fell more nearly along a smooth curve than did those plotted against a $Z-Z_p$ calculated on the basis of the postulate of Pappas. Accordingly, the curve used by Gibson was redrawn to integrate more nearly to unity (Gibson's curve integrates to 0.90), and was used to calculate the mass-yield corrections used in this work. The experimental curve is shown in Figure 3, and an integrated curve based on it in Figure 4.

To calculate Z_p, it was necessary to have some idea of how many neutrons were emitted during the fission process. An estimate of $\bar{\upsilon}$, the average number of neutrons emitted, was made by using the formula

$$\bar{\upsilon} = 2 + E_{ex}/8,$$

where E_{ex} is the excitation energy of the compound nucleus in Mev. The basis of the formula is that about two nuetrons are emitted in spontaneous fission[58] and an additional neutron is emitted for each additional 8 Mev of excitation (4 to 6 Mev for the neutron binding energy and 2 to 4 Mev for the kinetic energy of the neutron). Except for the few cases in which $Z-Z_p$ was less than -1.0, and error of 1 or 2 neutrons in the value of $\bar{\upsilon}$ did not make an appreciable error in the correction factor.

---

* Note added in processing. The experimental evidence of Biller[49] and of Hicks and Gilbert[53] do not agree with this formula; the results based on its use are, therefore, of dubious value.

Fission Yields

The corrected and uncorrected values of the cross sections for the production of the various fission products at different energies are presented in Table III. Figure 5 shows six curves of total yield of a given isobaric chain plotted against mass number for six helium-ion energies from 23.5 to 44.3 Mev. Both experimental and reflected points are shown; the reflection was made about the point $(237 - \bar{\upsilon})/2$, where $\bar{\upsilon}$ was calculated from the formula on page 31. Strictly speaking, one should find the best point for reflection and from this calculate $\bar{\upsilon}$. However, considering the quality of the data, it seemed more reasonable to assume a value of $\bar{\upsilon}$. For convenience of comparing the fission-yield curves, they have been replotted together in Figure 6, without the experimental points. Some of the points shown in Figure 5 were taken from plots of isobaric yield versus helium-ion energy, such as those shown in Figure 7.

Total Spallation and Fission Yields

The total fission cross section at a given energy is equal to the sum of all the individual fission-product cross sections (taken from the smooth curves of Figure 6) divided by two (since two fragments are produced in each fission event). Similarly, the total spallation cross section is the sum of the individual spallation cross sections at a given energy. The total fission and total spallation cross sections together with the percent spallation are plotted against helium-ion energy in Figure 8, and the total reaction cross section (sum of the fission and spallation cross sections) is shown plotted against helium-ion energy in Figure 9. Also shown in Figure 9 are two theoretical curves of the total reaction cross section calculated by Glass[59] on the basis of material given by Blatt and Weisskopf.[60] The upper curve has been calculated by using the radius parameter $r_o = 1.5 \times 10^{-13}$ cm, and the lower using $r_o = 1.3 \times 10^{-13}$ cm.

Sources of Error

The sources of error can be divided into two classes: one we call "absolute" errors because they are the same throughout all the bombardments; the other we call "relative" errors, because they may vary from bombardment to bombardment.

Table III

Corrected (C) and Uncorrected (U) Fission-Product Yields (millibarns)

E (mev)	Sr^{89}		Sr^{91}		Zr^{95}		Zr^{97}		Mo^{99}		Ru^{103}		Ru^{105}		Ru^{106}		Ag^{111}		Cd^{115}		Ba^{135m}		Ba^{139}		Ba^{140}		Ce^{141}		Ce^{143}		Ce^{144}		Nd^{147}		Eu^{156}		Eu^{157}		Tb^{160}		Tb^{161}	
	U	C	U	C	U	C	U	C	U	C	U	C	U	C	U	C	U	C	U	C	U	C	U	C	U	C	U	C	U	C	U	C	U	C	U	C	U	C	U	C
20.3																			0.18	0.19			0.54	0.78	0.52	0.90														
23.0							0.55	0.60	1.42	1.43			2.14	2.21			0.29	0.29																						
23.5					2.4	2.5	6.5	7.10			4.8	4.8	3.2	3.3					3.30	3.40			4.6	6.7	3.4	5.9	10.1	10.9	8.4	10.1	2.1	3.1	2.0	2.1			0.04	0.07				
26.2					11.5	11.9	14.8	16.6											9.91	10.3	0.42	4.0	9.24	16.1	7.38	16.8														
27.8					16.7	17.2	16.8	17.2											15.0	15.6							26.2	29.1	12.9	17.2	7.96	13.8	7.92	9.21	0.68	2.44	0.94	1.92			0.50	0.77
28.9											11.2	11.3	14.7	15.3	14.4	15.5			22.4	23.3	1.17	11.1	15.6	27.1	11.4	25.9														
30.7					21.2	22.2	12.0	14.1											32.4	34.5							13.2	15.2	12.0	17.6	8.76	17.9								
31.8																			28.9	30.7	3.39	21.5	23.4	47.8	14.9	41.4														
32.4							12.0	14.1	29.9	30.5			72.4	76.2			28.4	29.0																						
35.3	15.9	16.2	19.3	21.2	39.2	41.0	37.5	44.1			24.0	24.2	26.9	28.3	26.8	29.5			41.3	43.9	4.94	31.3	18.2	37.1	12.2	33.9														
36.8					28.1	29.7	22.2	27.1											46.1	50.1							11.8	14.2	18.7	32.5	7.33	20.4								
37.8			8.30	9.22							17.5	17.8	20.6	22.1	24.3	27.6			52.1	56.6	4.54	29.2	16.7	41.8	12.5	47.5														
40.4					45.5	48.1	44.8	54.6																			38.5	46.4			14.5	40.3	14.9	21.9	0.44	1.61	0.44	1.61	0.43	0.75	0.7	1.77
41.0	9.87	10.2	16.7	18.6	41.5	43.9	42.6	52.0											43.3	47.1	4.03	21.5	12.2	30.5	8.4	31.9							2.96	4.35						
43.8					42.3	44.8	34.9	42.6											70.5	76.6							15.6	18.8	27.0	47.0	15.5	43.1								
44.3	31.5	32.5	52.3	58.1	54.9	58.1	43.4	52.9			28.0	28.4	40.9	44.0	45.0	51.1			68.3	74.2	8.47	45.2	22.0	55.0	14.2	53.6														
44.4							27.9	34.0	31.5	32.5			75.3	81.0			43.6	44.9																						
46.2																			81.3	90.3																				
46.2	21.7	22.4	34.6	39.8	56.5	61.1	47.8	61.3											73.5	81.7	4.92	21.9	24.9	83.0	15.7	82.6														

MUB-144

The absolute errors arise from uncertainties in the half life of U^{233} (0.6%);[61] in the geometry factors for the alpha counters (1% for the counters used to measure the target activities and 2% for the ionization chambers with 52% geometry),[62] in the various counting efficiencies (5% to 20%), beta corrections (probably nor worse than 10%), and alpha branching ratios (0% to 40%); and in the assays of the tracers and carriers used to determine chemical yields (1% for the neptunium and plutonium tracers and 1% to 5% for the fission-product carriers).

Relative errors are due to uncertainties in the activity of the target (1%), in the area of the target (5%, based on a 2% to 3% uncertainty in the diameter), chemical yield (1% to 10% for fission products and 3% to 10% for spallation products), the activity of the products (1% to 3% for fission products and 0.5% to 10% for spallation products), and the intensity of the cyclotron beam (0.5%).[63] In addition there are sources of error such as uncertainty in the length of the bombardment, variation of the beam, nonuniformity of the target, and variation of counting efficiencies with sample thickness whose contribution cannot be evaluated.

The numerical values given above are based on an error of 0.01 mg in weighings, of the square root of the total number of events in determinations of activity, of 0.2 of the smallest division of the ruler in measuring lengths; on the root-mean-square deviation of a value of which several determinations have been made; on a few estimated uncertainties; and on probable deviations quoted by others (see references).

Taking the square root of the sum of the squares of the various values, we get the numbers given in Table IV for over-all relative, absolute, and total error.

Table IV. Estimated error

	Spallation products (%)	Fission products (%)
Relative	6 – 15	5 – 12
Absolute	7 – 40	10 – 12
Total	9 – 43	11 – 18

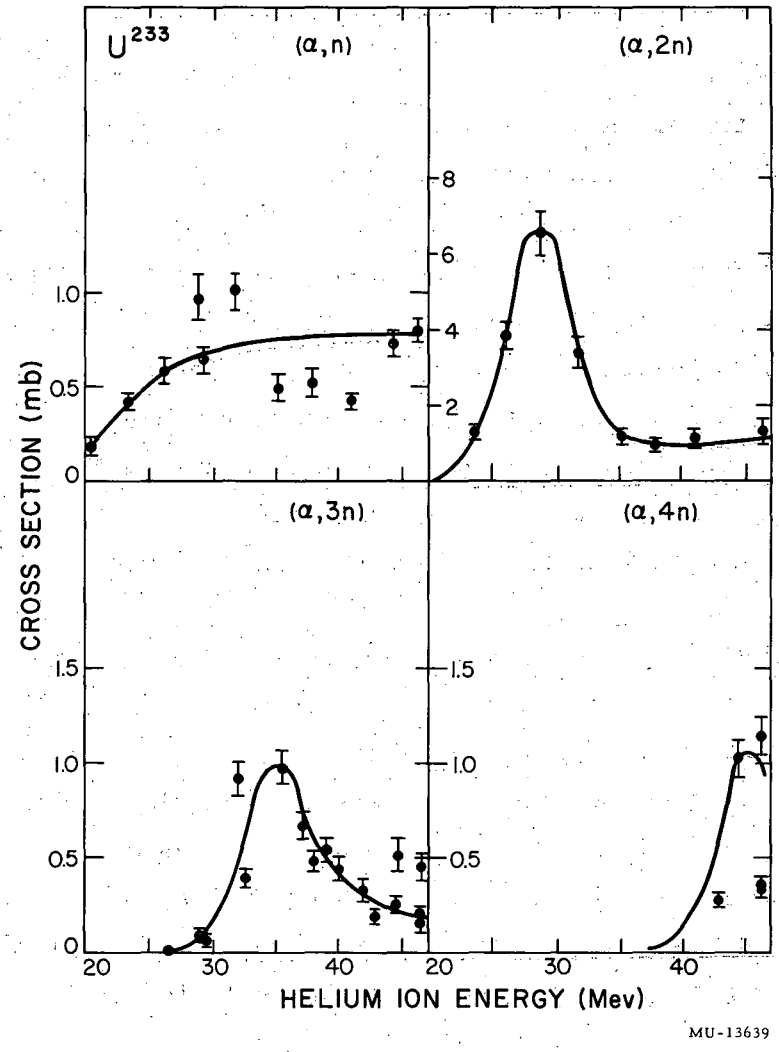

Fig. 1. The (a, xn) cross sections.

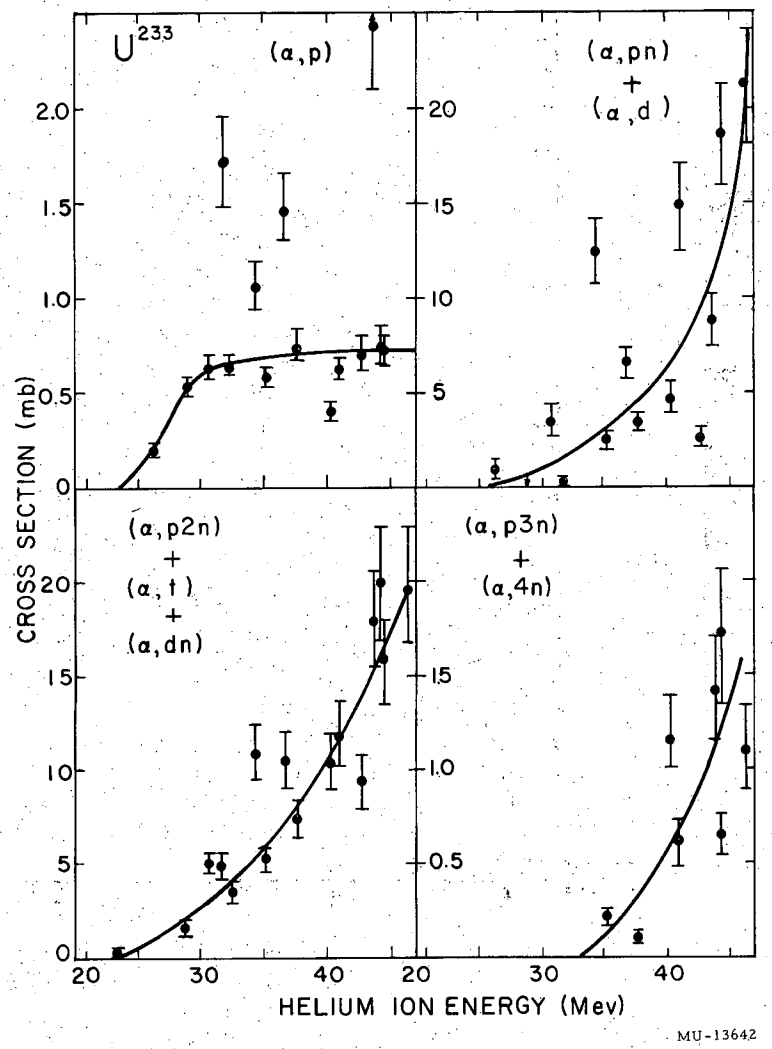

Fig. 2. The (α, pxn) cross sections.

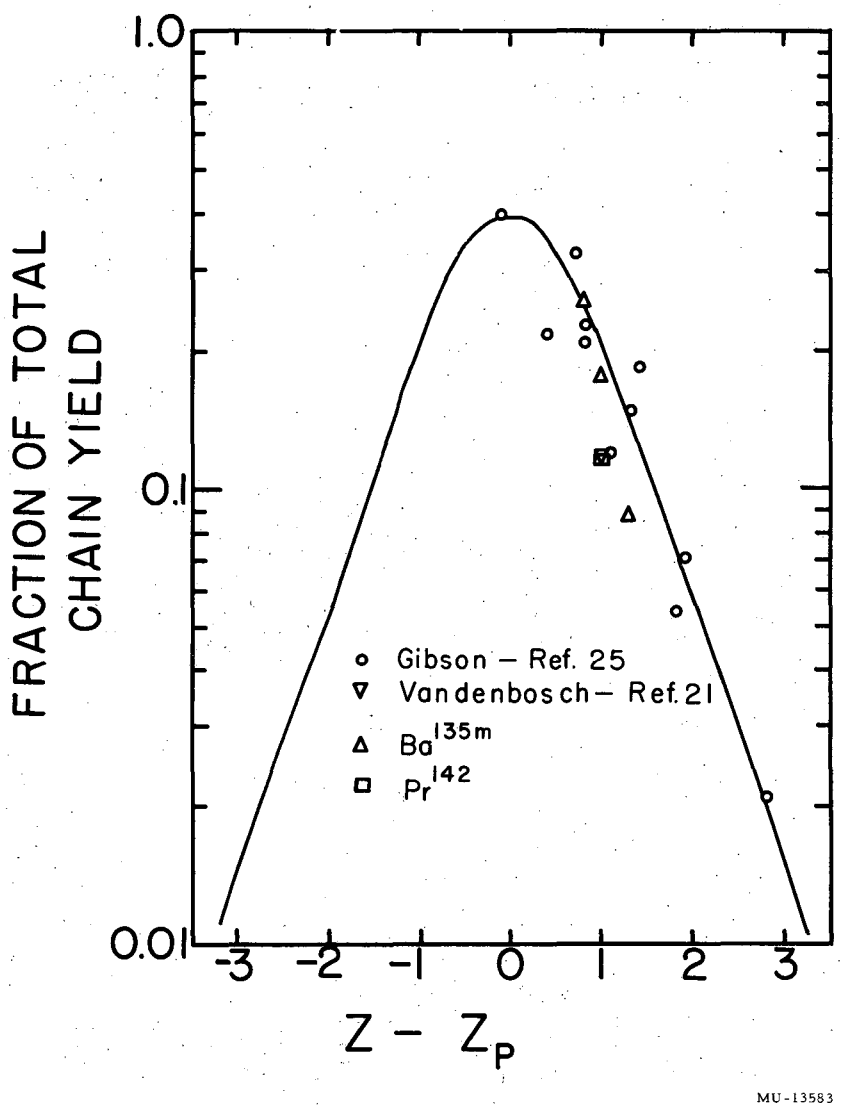

Fig. 3. Fraction of chain yield as a function of $(Z - Z_p)$.

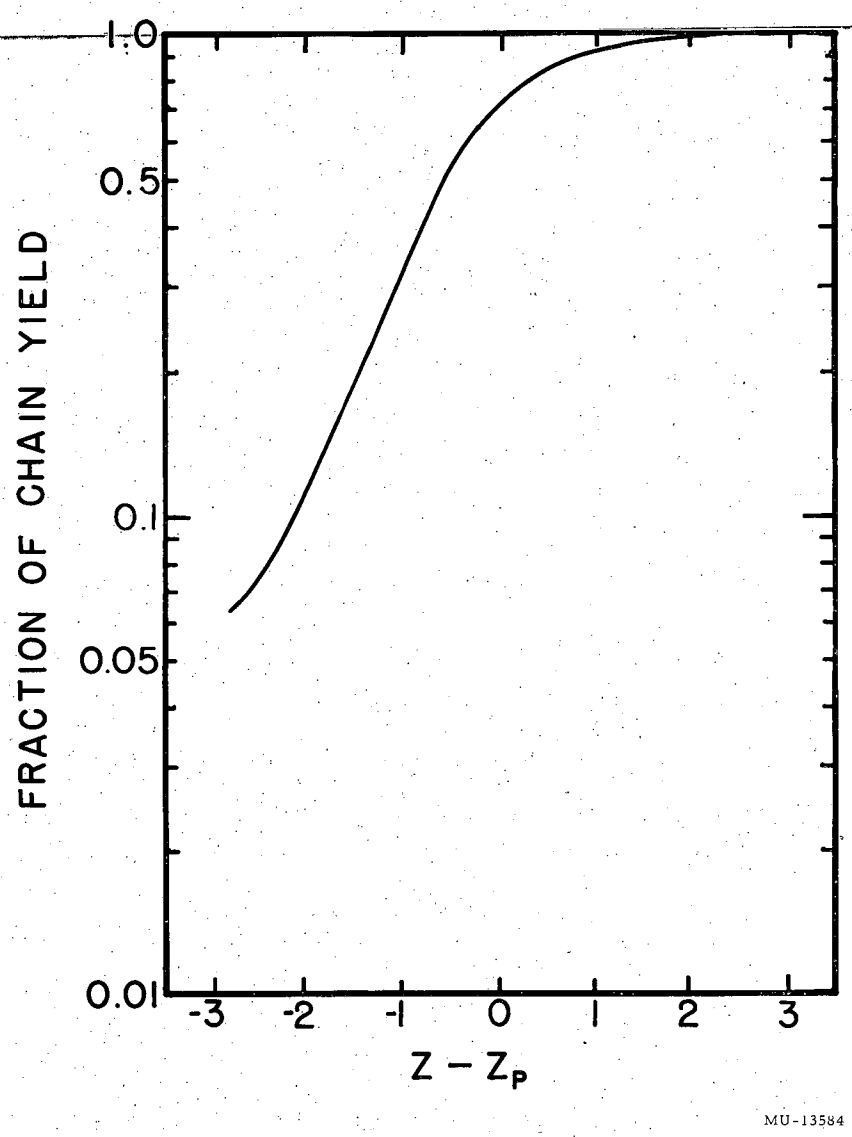

Fig. 4. Integrated fraction of chain yield as a function of $(Z - Z_p)$.

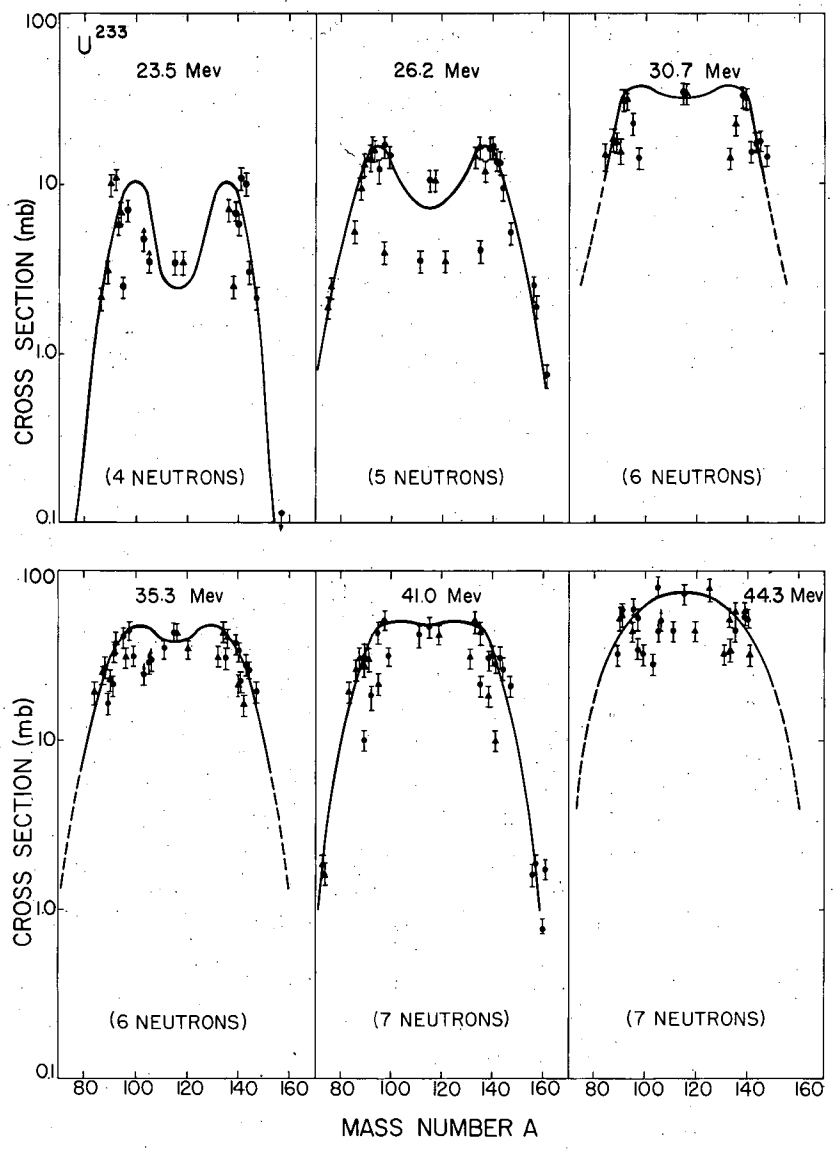

Fig. 5. Mass yield curves. ● - experimental points, ▲ - reflected points.

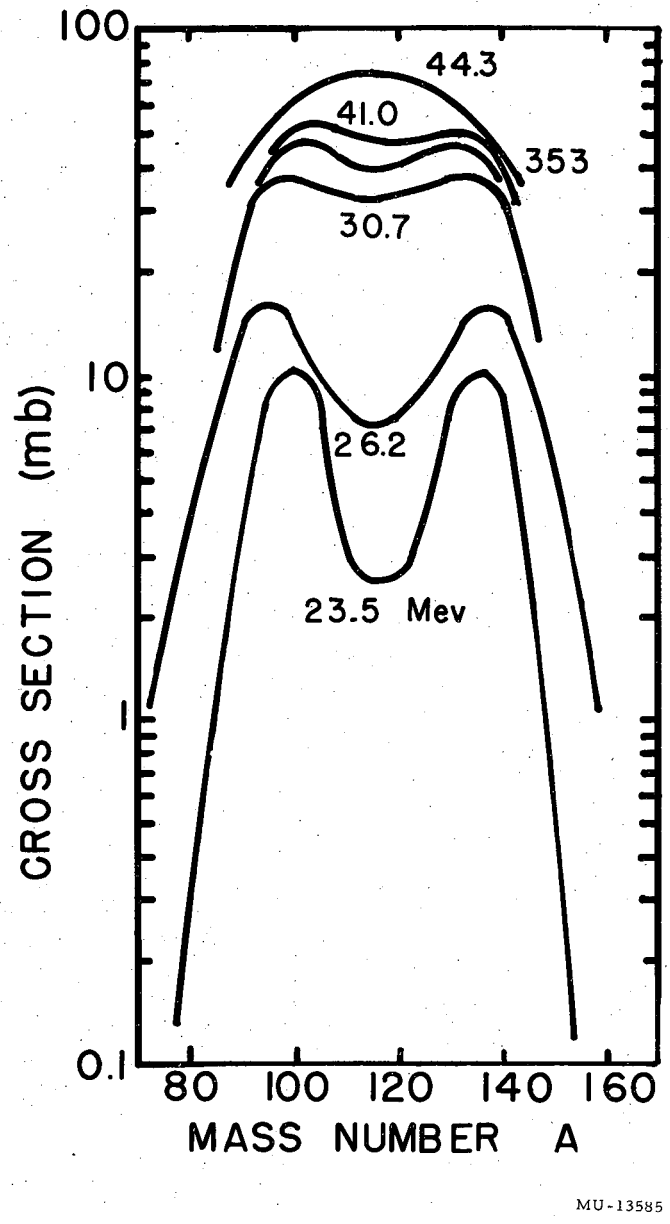

Fig. 6. Mass yield curves.

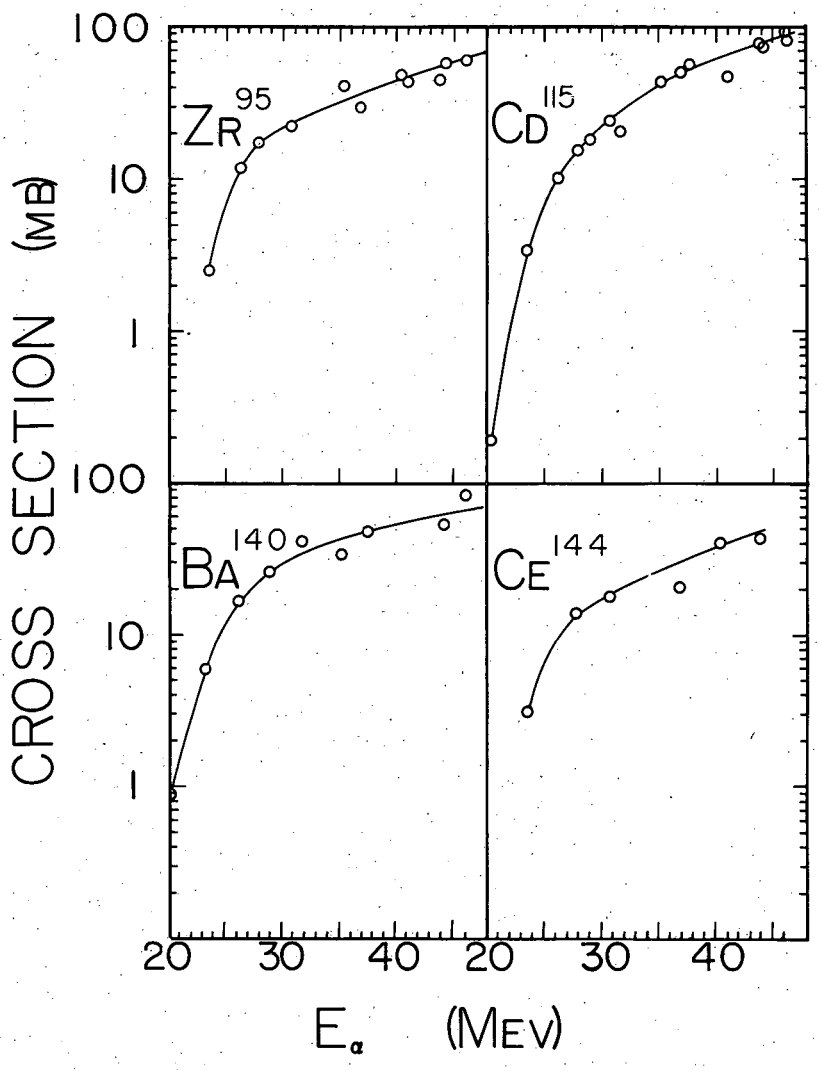

Fig. 7. Selected isobaric yields as a function of helium-ion-energy.

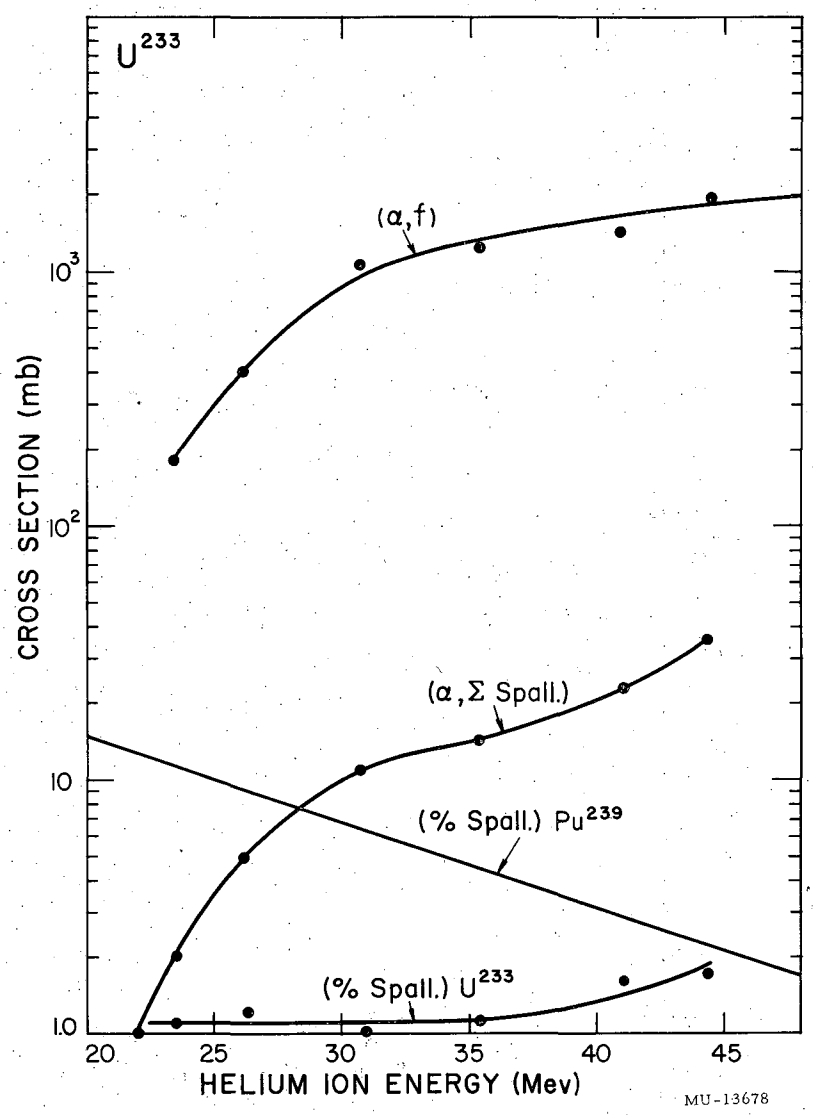

Fig. 8. Total fission and total spallation cross sections for U^{233} as a function of energy. Ratio of spallation to total cross section for U^{233} and Pu^{239}.

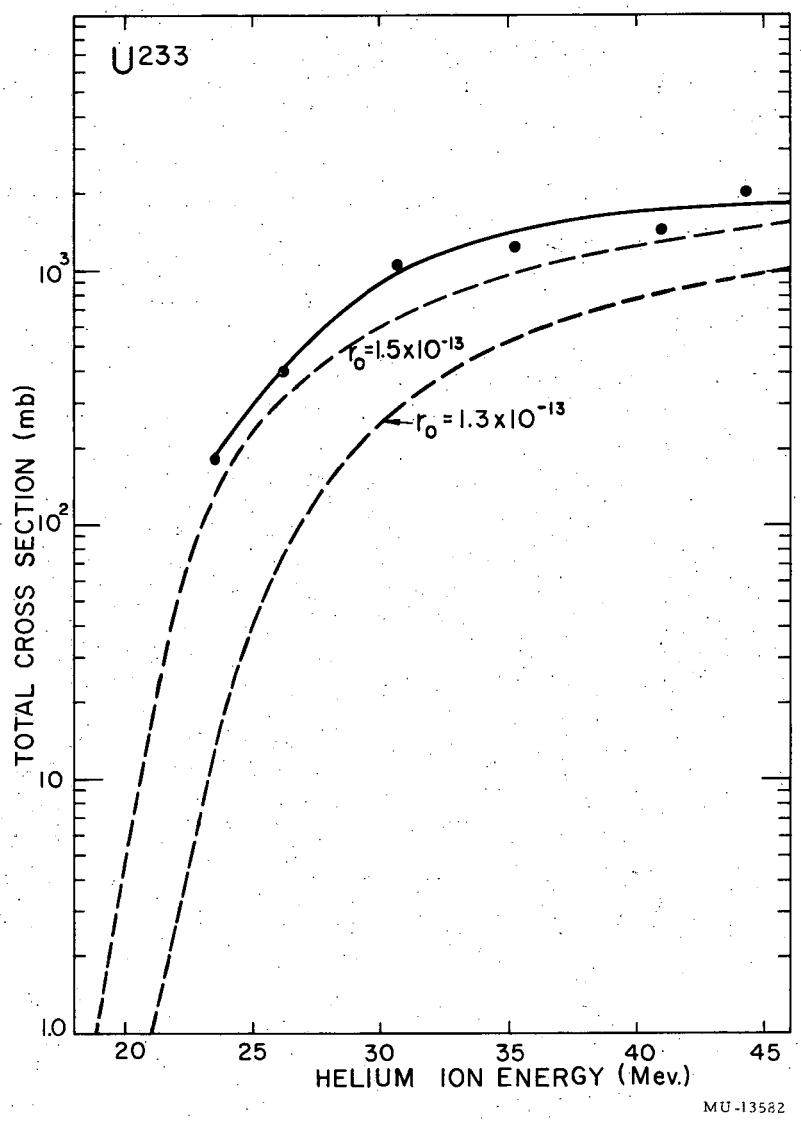

Fig. 9. Total reaction cross section as a function of energy.

IV. DISCUSSION

Features of the U^{233} Cross Sections

Spallation

The excitation functions for the spallation reactions induced in U^{233} with helium ions are marked by two striking characteristics: the cross sections for the (α,xn) reactions are very low, with the highest no more than 7 mb, and the cross sections for the (α,pxn) reactions are by contrast relatively high, rising in two cases to almost three times the height of the highest (α,xn) cross section. Other noteworthy features are the flatness of the curves for both the (α,n) and (α,p) cross sections, the peaks for the $(\alpha,2n)$ and $(\alpha,3n)$ cross sections, and the rapid rise of the (α,pn) and $(\alpha,p2n)$ cross sections, with no evidence that a maximum has been reached. (Perhaps at this point it should be stated that such expressions as "(α,pn)" do not necessarily mean that a proton and a neutron are emitted as individual particles, but rather that the product is one that would be formed if such particles were emitted.) Another interesting point is the sharp decrease in peak height between the $(\alpha,2n)$ curve and the $(\alpha,3n)$ curve.

These excitation functions show both similarities and contrasts to those of Pu^{239},[19] Pu^{238},[19] and U^{238}.[20] In general, the shapes of the curves in all four cases are similar -- flat (α,n) and (α,p), peaked $(\alpha,2n)$ and $(\alpha,3n)$, and sharply rising (α,pn) and $(\alpha,p2n)$ curves. Also, the (α,xn) cross sections show a similar decrease in peak height for succeeding value of x. The major dissimilarity is that the magnitude of the (α,xn) cross sections for U^{233} are considerably lower than those for the other nuclides. In particular, we note in Figure 8 that the ratio of the total spallation cross section to total reaction cross section for Pu^{239} is about 10% at the lowest energy and decreases to about 2% at the highest energy. The same ratio for U^{233}, on the other hand, remains close to 1% at nearly all energies, rising to a little more than 1.5% at the highest energies.

Glass, Carr, Cobble, and Seaborg have explained the lowness of their cross sections by saying that both fission and the major part of the (α,xn) reactions go by way of a compound nucleus and that fission

competes more successfully than does spallation to claim the larger share of the total cross section.[19] The decrease in the peak heights for the successive (α,xn) reactions in interpreted to mean that fission is competing successfully at every step of the evaporation to cut down on the number of remaining compound nuclei. The long tails on the (α,xn) excitation functions and the relatively high cross sections for the reactions involving the emission of charged particles suggest that there are direct interaction mechanisms by which a projectile can interact with a few nucleons on the nuclear surface, knocking out one or more of them, without leaving much of its energy in the nucleus, with the result that the residual nucleus is not sufficiently excited to undergo fission. Hence, the products of the direct-interaction-type reactions survive, whereas the products that result from the formation of a compound nucleus tend to be eliminated by fission. It has been further suggested by Glass and co-workers that reactions such as the (α,p2n) occur with the emission of a high-energy triton. Work by Wade, Gonzalez-Vidal, Glass, and Seaborg has shown that high-energy tritons are indeed emitted when U^{238} is bombarded with helium ions.[31] Calculations based on a classical model for this reaction, given in Appendix C, show that if the model is valid, the residual nucleus will have an excitation of only a few Mev.

The excitation functions that have been measured for U^{233} can be readily explained in terms of the above theory. From the factor-of-ten difference between the ratio of spallation to total cross section in U^{233} and that in Pu^{239}, we must conclude that fission is competing even more successfully in the reactions of U^{233} than in the reactions of Pu^{239}. (Gibson has reached the same conclusion on the basis of his work on the deuteron-induced reactions of U^{233} and Pu^{239}.)[25] The spallation reactions involving the formation of a compound nucleus have been so drastically reduced in U^{233} by fission competition that the majority of the observed reactions are due to direct interactions. At the higher helium-ion energies, which favor the direct interactions, these reactions have increased so much relative to the compound-nucleus reactions that the ratio of spallation to total cross section has actually increased. In Pu^{239}, on the other hand, where at low energies the compound-nucleus

spallation reactions survive relatively well, the increase in excitation with increasing helium-ion energy causes fission to compete more successfully against the other compound-nucleus reactions, with the result that the cross sections for these reactions decrease faster than the direct-interaction cross sections increase. The result is that the ratio of spallation to total cross section decreases with increasing energy.

For U^{233} and Pu^{239} bombarded with deuterons, cross sections for the spallation reactions of Pu^{239} again run higher than those for U^{233}, although the difference is not so marked as in the helium-ion-induced reactions.[25] Since the deuteron is a particle particularly susceptible to direct-interaction-type reactions, it seems likely that a large portion of the deuteron-induced reactions go by this mechanism. The products from such reactions then survive fission equally well in either case. The observed differences in the magnitudes of the cross sections for corresponding deuteron-induced reactions on the two nuclides are attributable to that part of the spallation reactions that goes by way of a compound nucleus, with the resulting elimination by fission of most of the products.

Fission

The determination of the individual fission-product cross sections was undertaken with the view of determining the total fission cross section; the data are barely good enough for that purpose. One is not justified in trying to draw any conclusions regarding the characteristics of the fission reaction on the basis of these curves. It is sufficient to note that, as in most of the spallation-fission studies, fission induced by low-energy helium ions is asymmetric, and fission induced by high-energy helium ions tends to by symmetric.

An interesting point with regard to fission yields has been made by Fong.[64] If the fissioning nucleus has an even mass number A, the total yield at mass A/2 is just twice that at mass A/2 + 1 or A/2 - 1, since two identical particles rather than two different particles are formed in the fission. The emission of neutrons during and after the fission process tends to spread out the increased yield over several

mass numbers, causing the effect to be less noticeable. In high-energy fission there are several different compound nuclei fissioning (one for each stage of neutron evaporation), and there is additional smearing out of the raised yield. I believe that in this work the experimental uncertainties are too great for such an effect either to be noticeable or to contribute any appreciable additional uncertainty to the values of the fission cross sections.

Total Cross Section

A comparison of the measured total cross section with the calculated cross section – shown in Figure 9 – indicates that the correct radius parameter is slightly larger than $r_o = 1.5 \times 10^{-13}$ cm. This figure is in agreement with that determined by Gibson from the results of his deuteron bombardments of U^{233}, and is in general agreement with those determined by others doing similar experiments at this laboratory.[19,20,25]

The Compound-Nucleus Reactions

The Effect of Neutron-Binding Energies

If we accept the explanation that the spallation reactions of U^{233} proceding by way of a compound nucleus are cut down by fission more than are the same reactions in Pu^{239}, we have not solved the problem, but have merely replaced it by another one: why does fission compete more successfully in the reactions of U^{233} than in the reactions of Pu^{239}? The two target nuclides are the same nuclear type and are the same distance from the line of beta stability. Furthermore, Pu^{239} has a slightly larger Z^2/A than does U^{233}; on this basis, we would expect fission to compete more successfully in Pu^{239} than in U^{233}.

Carr has suggested a theory that leads to a partial explanation of the paradox.[65] He has postulated that neutron emission is fast with respect to fission and fission is fast with respect to gamma emission. Hence, if the excitation energy of the nucleus is greater than the binding energy of the last neutron, a neutron is in general emitted. If the excitation energy after all the neutrons have been emitted is above the fission threshold, the nucleus fissions. If the excitation energy after

all the neutrons have been emitted is below the fission threshold, the nucleus de-excites by gamma emission. It follows, therefore, that the ease with which a given reaction can compete against fission depends upon the energy spacing between the fission threshold and the binding energy of the last neutron of the reaction product. Jackson has proposed a similar theory in which the outcome of the competition between neutron emission and fission depends on this energy spacing.[66]

The drawback to Carr's theory is that it makes no allowance for fission competition at the various stages of neutron evaporation. Glass, Carr, Cobble, and Seaborg have concluded that fission competes at every step.[19] However, we can use this theory to give a partial explanation of why fission competes more successfully in the U^{233} reactions than in the Pu^{239} reactions. Let us consider the nucleus that has survived fission long enough that it has evaporated all the neutrons that the original excitation would allow. The excitation energy of this nucleus must be less than the binding energy of the last neutron. Because of the increase of the level density with excitation, the most probable excitation energy will be close to the neutron-binding energy. Furthermore, for excitations of this magnitude, the level width for fission is almost certainly a sensitive function of excitation, increasing rapidly with increasing excitation. Thus, a high neutron-binding energy implies a high excitation energy for the residual nucleus; a high excitation implies a high level width for fission. Hence, those products having a high binding energy for the last neutron will be less likely to survive than those having a low binding energy. If we compare the neutron-binding energies for isotopes of plutonium and curium (in Table V), we see that for analogous nuclei – that is, those nuclei that are separated by two protons and four neutrons and are, in this case, products of the same reaction in the two different targets – the plutonium isotopes have higher binding energies than do the curium isotopes.

Table V

Binding energy of the last neutron in plutonium and curium isotopes

	(Mev)		
Pu^{237}	6.05	Cm^{243}	5.66
Pu^{236}	7.39	Cm^{242}	6.99
Pu^{235}	6.21	Cm^{241}	6.13
Pu^{234}	7.67	Cm^{240}	7.51
Pu^{233}	6.36	Cm^{239}	6.34

Values taken from Regerence 58.

Another factor to be considered is the so-called fission "threshold." However, curves given by Jackson indicate that analogous nuclei in this region have approximately the same fission threshold.[66,67]

Jackson's Model

Jackson[68] has proposed a model for spallation reactions that combines the results of the Monte Carlo calculations by McManus, Sharp, and Gellmann and by McManus and Sharp[69] with a formula giving the probability of evaporating a given number of neutrons from a nucleus with a given excitation. The result is a model that takes into consideration the effects of both direct interaction and evaporation.

According to Jackson, the probability that a nucleus with excitation E will emit exactly x neutrons is

$$P(E,x) = I(\Delta_x, 2x-3) - I(\Delta_{x+1}, 2x-1) ,$$

where I(z, n) is Pearson's incomplete gamma function,

$$I(z,n) = \frac{1}{n!} \int_0^Z x^n e^{-x} dx ,$$

and $\Delta_x = (E - \sum_i^x B_i)/T$. B_i is the binding energy of the ith neutron and T is the nuclear temperature, which is assumed to be constant.

Although it is doubtful that the results of the Monte Carlo calculations, which were made for bombardments with protons, can be extended to give more than approximate results for bombardments with

helium ions, the formula for calculating the probability of neutron evaporation is valid regardless of the projectile. Even without considering the effect of fission, it is possible to estimate within a few Mev the position of the peak for a given reaction in the very heavy elements.

However, a modification can be made to the evaporation formula to include the effect of fission competition so that the formula can be used to calculate the cross sections for reactions proceeding by way of a compound nucleus. The modified expression is

$$\sigma(\alpha,xn) = \sigma_c \overline{(\Gamma_n/\Gamma_t)}^{x} \left[I(\Delta_x,\ 2x-3) - (\Gamma_f/\Gamma_t)\ I(\Delta_x^f,\ 2x-1) - (\Gamma_n/\Gamma_t)\ I(\Delta_{x+1},\ 2x-1) \right],$$

where $\sigma(\alpha,xn)$ is the cross section for the (α,xn) reaction at a given energy, σ_c is the total reaction cross section at that energy, $\overline{(\Gamma_n/\Gamma_t)}$ is an average ratio of neutron level width to total level width, $\Delta_x^f = (E - \sum_i^x B_i - E_{th})/T$, where E_{th} is the fission threshold for the residual nucleus. The following assumptions are made to simplify the calculations:

1. $\overline{(\Gamma_n/\Gamma_t)}$ is independent of energy .

2. $(\Gamma_n/\Gamma_t) + (\Gamma_f/\Gamma_t) = 1$. That is, reactions other than neutron emission are negligible.

3. $(\Gamma_f/\Gamma_t) = 1$ for $(T\Delta_{x+1}) < 0$,

   $(\Gamma_f/\Gamma_t) = 1 - (\Gamma_n/\Gamma_t)$ for $(T\Delta_{x+1}) > 3$ Mev, and

   (Γ_f/Γ_t) is obtained by linear interpolation between the above two values for $0 < (T\Delta_{x+1}) < 3$ Mev. The bases of these assumptions are that for excitations between the fission threshold and the binding energy of the last neutron, the nucleus will almost certainly fission; that for moderate excitations more than a few Mev above the binding energy of the last neutron, Γ_n/Γ_f is probably constant; and that Γ_f/Γ_t reaches its constant value about 3 Mev above the neutron-binding energy. The two parameters $\overline{(\Gamma_n/\Gamma_t)}$ and T are to be determined.

An explanation of the various terms in the formula will make its "derivation" more understandable. The factor $\overline{(\Gamma_n/\Gamma_f)}_x$ is to correct for the nuclei that are destroyed by fission of the x compound nuclei existing at the various stages of evaporation. The expression $I(\Delta_x, 2x-3)$ is the probability that at least x neutrons will evaporate from the compound nucleus with excitation E; $I(\Delta_x^f, 2z-1)$ is the probability that the nucleus remaining after the evaporation of x neutrons will have enough energy to fission, and $I(\Delta_{x+1}, 2x-1)$ is the probability that the nucleus will have enough energy to emit another neutron. The term Γ_f/Γ_t and Γ_n/Γ_t are weighting factors to account for the relative probabilities of fission and neutron emission.

The cross sections for the (α,xn) reactions of U^{233} and Pu^{239} have been calculated by use of this method. The results are shown in Figures 10 and 11. In both cases T was equal to 1.5 Mev; for U^{233} $\overline{(\Gamma_n/\Gamma_t)}$ = 0.13 and for Pu^{239} $\overline{(\Gamma_n/\Gamma_t)}$ = 0.19. The fission thresholds used were 4.5 Mev for even-mass nuclides and 5.1 Mev for odd-mass. The fit of the curves to the data is far from quantitative, but it is remarkable that such a simple model gives as good a fit as it does. The chief weakness of the model is that Γ_n/Γ_f is almost certainly not a constant. Vandenbosch[21] has proposed a modification that takes into consideration the variation of Γ_n/Γ_f with mass number and with nuclear type. The agreement with the experimental points is considerably improved.

The model is good enough, however, that we can conclude that the long tails on the curves representing the (α,n) and $(\alpha,2n)$ cross sections are due largely to some direct interaction. Of this more will be said below.

The Direct Interactions

Introductory Remarks

The possibility of a direct interaction between the projectile and the individual nucleons of the target has been recognized for several years. Serber proposed that at high bombarding energies the mean free path of the projectile is long compared with nuclear dimensions and that the nucleus is therefore partly "transparent."[70] An incoming high-energy

particle might knock out one or more nucleons directly without the formation of a highly excited compound nucleus. Butler has discussed the deuteron-stripping and pickup reactions, in which either an incident dueteron is stripped of one of its particles, or an incident proton (or neutron) pickus up a neutron (or proton) to form a deuteron.[71]

In general, one expects to see the effects of direct interaction only at projectile energies greater than 50 Mev. In the reactions of nonfissionable nuclei, the prominent compound-nucleus spallation reactions generally mask any small effects due to direct interaction. The region of fissionable nuclides is, therefore, a particularly good place to study direct interaction reactions with fairly low-energy particles, because the reactions going by way of a compound nucleus are largely eliminated by fission competition. Butler contends that most of the reactions that populate low-lying levels in the residual nucleus are formed by direct reactions;[72] we may add that most of the residual nuclei that have high excitations are destroyed by fission. Hence, most of the surviving products of spallation reactions in the region of fissionable nuclides are produced by direct interactions.

The Monte Carlo calculations by McManus, Sharp, and Gellmann and by McManus and Sharp,[69] as described by Jackson,[68] show that for 50-Mev incident protons on a heavy nucleus, less than half of the reaction cross section is accounted for by the production of a compound nucleus without the direct emission of any particles. In about one-third of the cases at this energy one neutron is knocked out directly. The validity of extrapolating the calculations made for protons so as to apply to reactions induced by helium ions is somewhat questionable, as also is the validity of the model upon which the Monte Carlo calculations are based for projectile energies of less than 50 Mev. However, it is fairly safe to say on the basis of these calculations that some few percent of the reactions involve the direct emission of a neutron. Furthermore, if the reactions not involving direct interaction tend to be eliminated by fission, those that do involve direct interaction may well account for a considerable fraction of the observed cross section.

The Excitation Functions

(α,n) and (α,p). We see from the theoretical calculations illustrated in Figures 10 and 11 that if the (α,n) reaction occurred entirely by formation of a compound nucleus, we would expect the cross section to drop rapidly with increase in energy; it does not. Furthermore, we note that in the reactions of both U^{233} and Pu^{239} the (α,n) and (α,p) cross sections are of the same magnitude and the curves have the same shape. Evaporation theory predicts and experimental evidence indicates that in the region where fission does not compete, the (α,p) cross sections should be considerably lower than the (α,n). Since fission tends to eliminate the reactions involving a compound nucleus, and since both the (α,n) and (α,p) reactions survive equally well against fission, we conclude that the surviving products of these reactions have been formed by a non-compound-nucleus reaction.* The most reasonable mechanism is a knock-on, in which the helium ion strikes the nucleon, which is then emitted. A classical calculation shows that if we regard the nucleon as a free particle, the helium ion may give up as much as 16/25 of its energy to the ejected nucleon. If we assume that the neutron-binding energy comes from the other 9/25 of the projectile's energy, we see that even for helium ions with energies as high as 30 Mev, the nucleus may be left with less than 7 Mev of excitation. A simple stripping model is inadequate because of the difficulty of finding a mechanism by which the nucleus could be left with low excitation.

---

* An argument can be made that both the (α,n) and (α,p) reactions involve the formation of a compound nucleus. An (α,p) product will be formed only when enough energy is concentrated on one proton that it can pass over the barrier. An (α,n) product will survive only when the neutron carries off sufficient energy that the residual nucleus is at too low an energy to fission. The two processes are essentially identical, and we will expect the excitation functions to be similar. However, we see from the theoretical calculations that the probability of concentrating enough energy on one particle to leave the nucleus at a low excitation decreases rapidly with increasing initial excitation, whereas the observed cross sections are constant for almost all excitations.

(α,2n). The general agreement of the theoretical (α,2n) excitation functions with the experimental indicated that a large portion of the (α,2n) cross section is due to compound-nucleus formation. As in the case of the (α,n) cross sections, the failure of the curve to drop rapidly at higher energies implies that there is a contribution to the cross section from direct interactions. A likely explanation is that one neutron is knocked out as described above and a second neutron is evaporated. (The Monte Carlo calculations already mentioned indicate that the knocking out of one neutron is the most probable direct interaction up to 100 Mev). Many of the direct interactions to knock out one neutron will leave the nucleus with enough energy to evaporate a second neutron. Fission tends to cut down the products, but not so severely as it cuts down the products from the reaction involving the evaporation of two neutrons, since in the latter case fission has two chances to compete with neutron emission whereas in the former it has only one. The fact that the tail on the (α,2n) excitation function for U^{233} is lower than that for Pu^{239} is evidence of the increased fission competition at the evaporation stage of the reactions of U^{233}. A comparison of the (α,2n) excitation functions for the two heavy elements with those of bismuth shows that the peaks have been cut down by fission more than have the tails,[73] an observation that lends further support to the idea that the peaks, being due to initial compound-nucleus formation, suffer from fission competition twice, whereas the tails, being due partly to direct interaction, suffer from fission competition only once.

(α,3n) and (α,4n). There is no experimental evidence for any direct-interaction contribution to the (α,3n) and (α,4n) cross sections, as would be expected. The Monte Carlo calculations indicate that the direct knocking out of three neutrons does not begin until the kinetic energy of the projectile reaches 50 Mev, and that below this energy the probability of the direct removal of two neutrons is small. Hence, the only remaining mechanism involving direct interaction is the direct emission of one neutron, followed by the evaporation of two (or three) more. Since two (or three) steps of these reactions involve evaporation, we

expect the excitation functions to be almost indistinguishable from those for the evaporation of three (or four) neutrons and also expect the products to have been cut down severely by fission.

(α,pn) and (α,p2n). The evidence is overwhelming that the products of the (α,pn) and (α,p2n) reactions of the heavy elements are produced almost entirely by the direct emission of high-energy deuterons or tritons, without the formation of a compound nucleus.

Wade, Gonzalez-Vidal, Glass, and Seaborg have measured the production of tritium in U^{238} bombarded with helium ions and have shown that the amount produced is approximately equal to the amount to be expected if the entire cross section for the (α,p2n) reaction -- measured radiochemically -- is due to the (α,t) reaction.[31] Furthermore, in a series of bombardments of elements throughout the periodic table, they have found that for elements of low Z the emitted tritons have low energies and are probably produced by a compound-nucleus mechanism, whereas for elements of high Z the emitted tritons have high energies and are probably produced by direct interaction.[74]

That the (α,pn) and (α,p2n) cross sections do not appear to suffer from fission competition is further evidence that a direct interaction leaving the nucleus with a low excitation is taking place. A comparison of the (α,pn) excitation functions of U^{233}, U^{238}, and Pu^{238} shows that they are all of the same magnitude, although the target nuclides vary greatly in fissionability – the cross section for the (α,4n) reaction in U^{233} is about 1 mb, in U^{238} about 60.[20] Amiel, Harvey, and Wade have recently measured the (α,pn) cross section of platinum, a nonfissionable nuclide, and found values close to those reported here for U^{233} – a further indication that fission is not competing against the (α,pn) reaction.[75] Similarly, the (α,p2n) excitation functions for U^{233}, U^{238}, Pu^{238}, and Pu^{239} are alike in both shape and magnitude.[19,20]

By comparing the (α,pn) and (α,p2n) with the (α,2n) and (α,3n) excitation functions, we can further eliminate the possibility that the former reactions occur appreciably by any other mechanism than the direct

emission of deuterons and tritons. We note that both the (α,pn) and $(\alpha,p2n)$ cross sections at full energy are about twenty times as great as the $(\alpha,2n)$ and $(\alpha,3n)$ cross sections. If the (α,pn) reaction took place by the emission of a separate proton and neutron, either by formation of a compound nucleus or by direct interaction, a similar mechanism should also cause the emission of two neutrons with at least equal frequency, with the result that the $(\alpha,2n)$ would be at least as large as the (α,pn) cross section. Similarly, except for the possibility of a direct interaction to emit a deuteron followed by the evaporation of a neutron, the only meachnism for the $(\alpha,p2n)$ reaction that could not work equally well for the $(\alpha,3n)$ is the direct emission of a triton. If the reaction were actually (α,dn), we would expect to see the curve of (α,d) excitation function turn downward at high energies because of the competition from the (α,dn) reaction.

The actual mechanism for the (α,d) and (α,t) reactions probably involves the stripping of a proton and a neutron in the former case and a proton in the latter, from a helium ion passing in such a way as to just touch the surface of the nucleus. A classical model for this mechanism is described in Appendix C.

$(\alpha,p3n)$. It is difficult to find a plausible mechanism for the $(\alpha,p3n)$ reaction. The most probable is the direct emission of a triton followed by the evaporation of a neutron. (The existence of a bound H^4 seems doubtful, and hence the emission of such a particle is unlikely.) If this were the case, however, we would expect to see a decrease in the (α,t) cross section at the energies at which the (α,tn) product begins to appear; no such decrease is observed. The data given in Table II and Figure 2 for the $(\alpha,p3n)$ cross sections have not been corrected for decay, during bombardment and prior to separation, of the parent, Pu^{233}, which is produced by the $(\alpha,4n)$ reaction. If we assume that the cross section for the direct production of Np^{233} by spallation is negligible, and calculate from the measured cross sections for this isotope the cross sections for the production of Pu^{233}, we find agreement within experimental error of the measured cross sections. (See Figure 12.) We conclude then that the direct production of Np^{233} is small, a conclusion

that is in keeping with the theory of the emission of complex particles by direct interaction. It is likely that at higher bombarding energies the residual nucleus from the (α,t) reaction will be left with sufficient excitation to evaporate another neutron, with the result that the (α,tn) reaction will become prominent.

Summary

1. Fission and the greater part of the (α,xn) reactions in U^{233} involve the formation of a compound nucleus.

2. The (α,pxn) reactions and, at high energies, the (α,xn) reactions involve direct interactions without the formation of a compound nucleus.

3. Fission competes so successfully with the other compound-nucleus reactions that the principal surviving reactions are those due to direct interactions.

4. Fission competes more successfully in U^{233} than in Pu^{239}. A partial explanation of this phenomenon can be given in terms of the higher neutron-binding energies for the products of the U^{233} reactions than for the products of the corresponding reactions of Pu^{239}. The explanation is not complete, however, since theoretical calculations indicate that fission is also competing more at every step of the evaporation process in the reactions of U^{233} than in those of Pu^{239}.

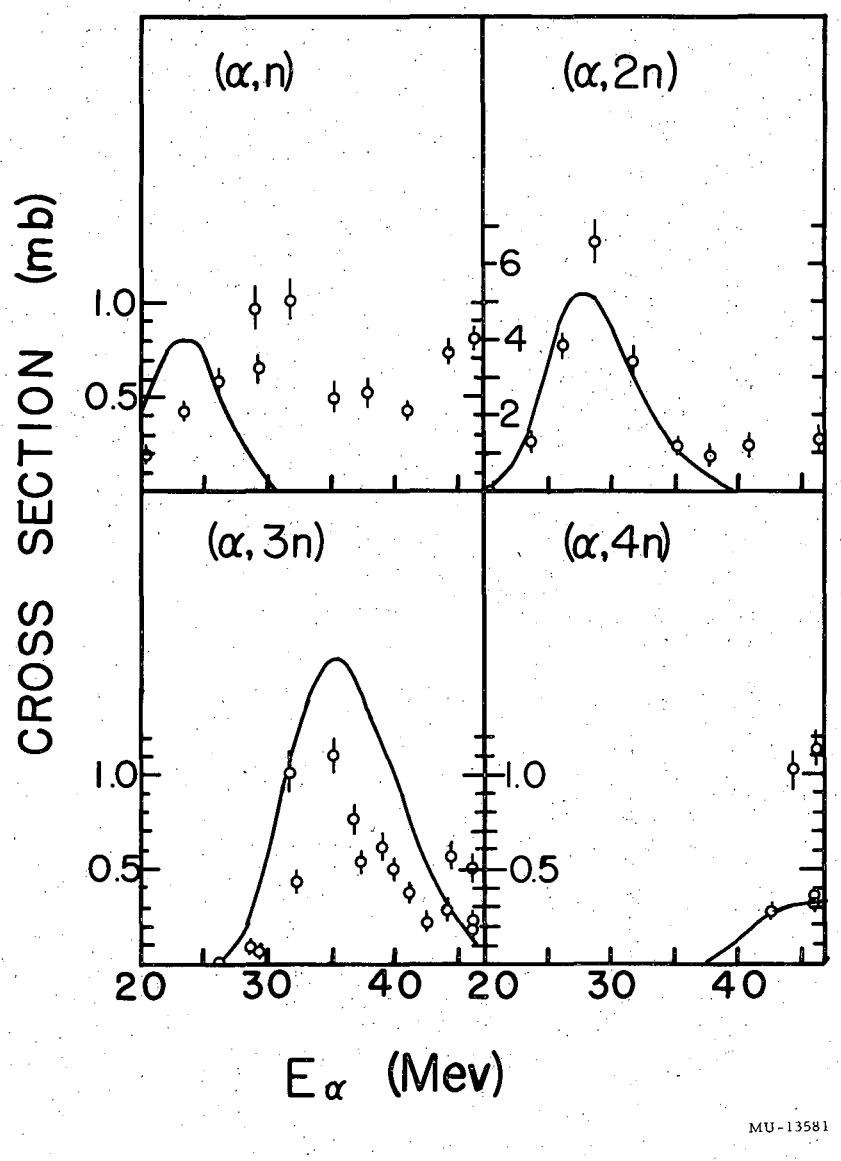

Fig. 10. Theoretical (a, xn) cross sections for U^{233}.

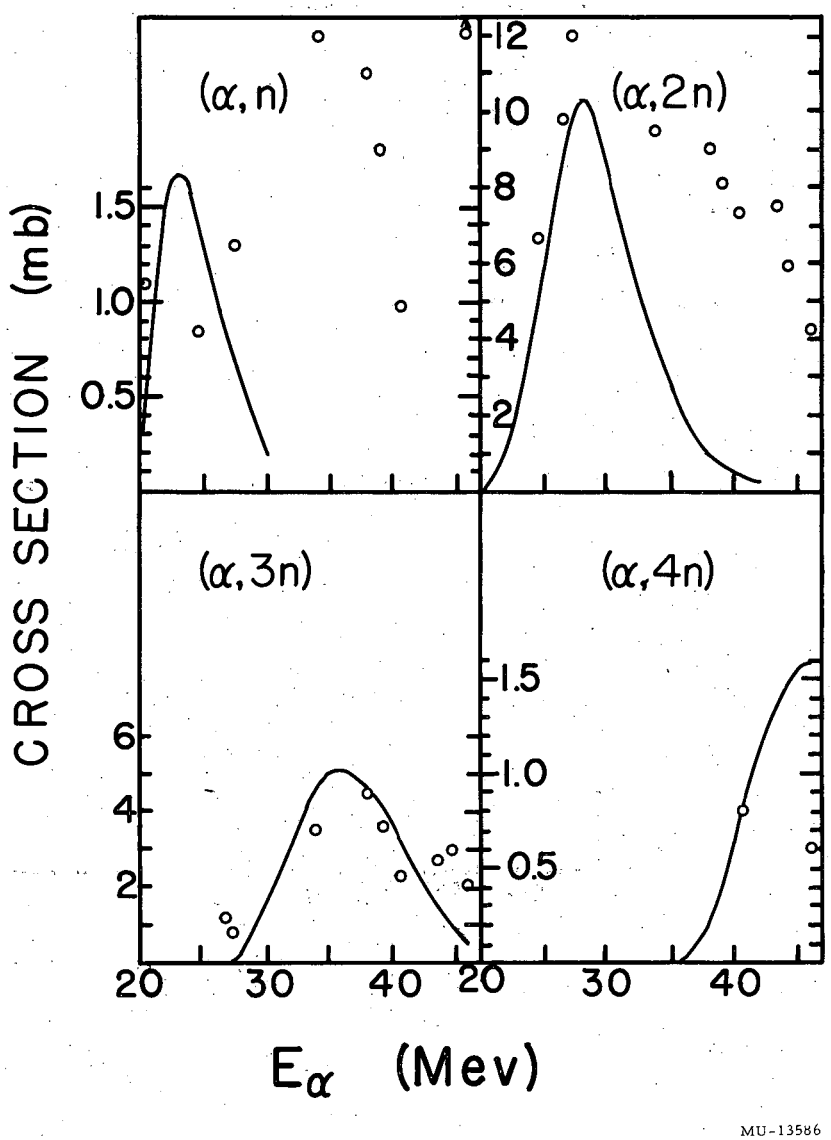

Fig. 11. Theoretical (a, xn) cross sections for Pu^{239}.

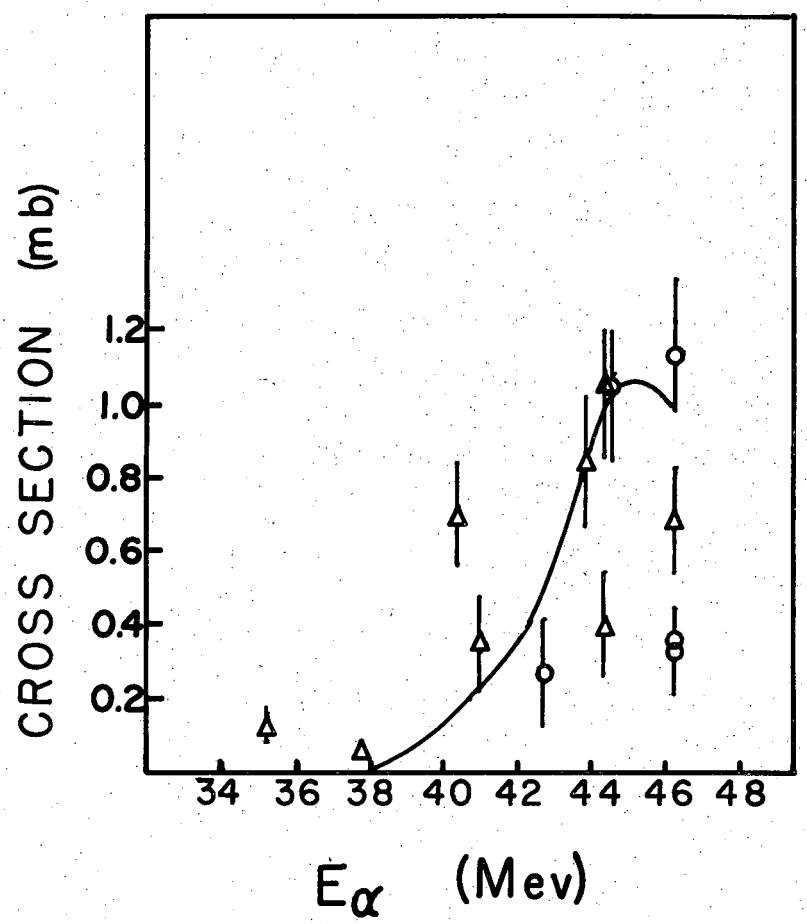

Fig. 12. Comparison of measured (α, 4n) cross sections to cross sections calculated from the yield of Np^{233}.

V. THE NEW ISOTOPE, PLUTONIUM-233[76]

A previously unobserved alpha activity, which is thought to be due to the decay of Pu^{233}, was detected in the pulse analyses of the plutonium fraction from five bombardments with helium ions of energies from 42.7 to 46.2 Mev. The channels at which the activity appeared correspond to an alpha-particle energy of 6.3 Mev, with an average of 6.30 ± 0.02 Mev. A pulse analysis from one bombardment is shown in Figure 13. The 6.30-Mev alpha peak disappeared in successive pulse analyses with a half life of about 20 minutes. Individual values ranged from 17.5 minutes to 24.1 minutes, with an average for the over-all half life of 20 ± 2 minutes. A typical decay curve is shown in Figure 14. The points have been corrected for background, for long-lived activity (9 hour) due to the high-energy edge of the adjacent Pu^{234} peak, and for contributions to the activity from the decay of Th^{226}, which grows in at 6.33 Mev[51] as a member of the Pu^{234} decay chain.

It was first thought that the observed alpha peak might be due to contamination by Th^{226}, which has an alpha-particle energy of 6.33 Mev and a half life of 31 minutes;[51] moreover, the appearance of Th^{228} (the daughter of U^{-232}) as a contaminant in the plutonium fraction seemed to confirm this possibility. However, a calculation made on the growth-and-decay analog computer (GADAC)[79] showed that the observed activity was greater than the amount of Th^{226} activity that could have "grown in" during the bombardment and separation time. In addition, it was shown in one bombardment that the amount of thorium following the plutonium chemistry was not more than 1% and was probably less than 0.1% of the total amount originally present in the target. Furthermore, in no bombardment were the decay products of Th^{226} observed. Finally, the fact that no 6.30-Mev alpha activity was observed below the threshold[78] for the $(\alpha,4n)$ reaction, where the cross section for the production of Pu^{234} (and, therefore, Th^{226}) is relatively high, is further evidence that the observed alpha particles cannot be due to Th^{226}.

The mass assignment is based primarily on three types of evidence: a rough excitation function, the appearance in the pulse analysis of alpha particles attributable to the U^{229} daughter of Pu^{233}, and the compatibility

of the alpha energy and half life with the alpha systematics.[51] The excitation function studies, which showed that the 6.30-Mev alpha activity was not observed when the bombarding energy was below or near the threshold for the $(\alpha,4n)$ reaction but well above the threshold for the $(\alpha,3n)$ reaction, indicate that the observed activity is probably not due to an isomer of the $(\alpha,3n)$ product, Pu^{234}. Furthermore, a small amount of 6.30-Mev alpha activity was produced in a bombardment below the threshold for the $(\alpha,5n)$ reaction, showing that this activity cannot be due to Pu^{232}. This latter experiment, however, was somewhat inconclusive. The pulse analyses following one bombardment showed the growth of an alpha activity of 6.42 Mev (the energy of U^{229}) [51] that corresponded approximately with the growth of U^{229} expected from the Pu^{233} alpha activity observed.

Experiments were also performed to isolate the Np^{233} daughter (which decay by electron capture with a 35-minute half life[47]) that was produced by the electron-capture decay of Pu^{233}, in order to determine the ratio of alpha disintegrations to electron-capture disintegrations of the new isotope, and, consequently, to determine the partial alpha half life of Pu^{233}. An extraction with thenoyltrifluoroacetone was made on an aliquot of the plutonium fraction, and the intensity of the radiations from the neptunium isolated was measured with the Nucleometer. In Figure 15 the decay of Np^{233} from one "milking" is shown. The electron capture disintegration rate of Pu^{233} was calculated from that of the Np^{233} activity which had "grown in," which was in turn calculated from the Np^{233} activity measured with the proportional counter, an assumed counting efficiency of 80%[79] for the measurement of the Np^{233} decay rate, and the extraction yield of the neptunium determined by the yield of Np^{237} tracer added to the plutonium before the milking. The ratio of the alpha disintegration rate to the total disintegration rate, or alpha branching ratio, thus obtained is $(1.2 \pm 0.5) \times 10^{-3}$, from which is calculated a partial alpha half life of 11 ± 4 days.

The alpha-particle energy and the alpha half life of Pu^{233} are in agreement with the values expected from the alpha-decay systematics[51,80] for an odd-mass plutonium isotope. The hindrance factor[51] for the alpha

decay of Pu^{233} calculated from the partial alpha half-life of 11 days is about 3.1, which is the same order of magnitude as the hindrance factors for the most favored decay of other odd-mass plutonium isotopes.[51] An inspection of the alpha-particle energies[51] of the most prominent alpha groups of odd-mass plutonium isotopes shows that they fall low on a plot of alpha energy versus mass number relative to the line joining their even-mass neighbors. (See Figure 16) The net result is a series of doublets in which the alpha energy of a particular odd-mass plutonium isotope is only slightly higher than that of the next heavier even-mass isotope. Pu^{233} and Pu^{234} exhibit this characteristic behavior.

It is also interesting to correlate the electron-capture-decay properties of Pu^{233} with half-life systematics.[81] Using the measured alpha disintegration energy of Pu^{233} (6.41 Mev); the measured alpha-decay energies[51] of U^{229}, Th^{225}, Ra^{221}, Em^{217}, At^{217}, Fr^{221}, Ac^{225}, Pa^{229}, and Np^{233}; and the negatron-decay energy of Bi^{213} [47] one can calculate (by the method of closed energy cycles)[78] an electron-capture decay energy of 2.1 Mev for Pu^{233}. Then, with the assumption that most of the electron-capture events proceed to the ground state of Np^{233}, the 2.1-Mev energy and 20-minute half life specify a log ft value of 5.6. This value is in the region of those corresponding to allowed transitions, although a value of 5.6 is not incompatible with the transitions being first forbidden. However, the conclusion that the transition is allowed correlates well with data on similar transitions in other heavy elements.[81]

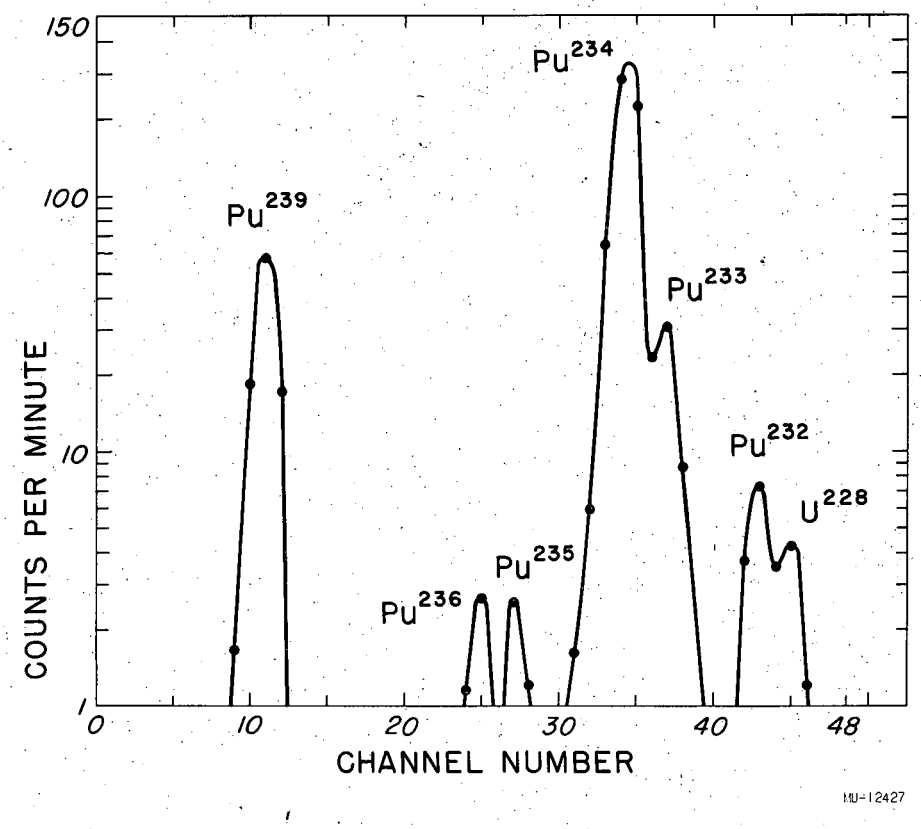

Fig. 13. Alpha pulse analysis showing peak due to the decay of Pu^{233}.

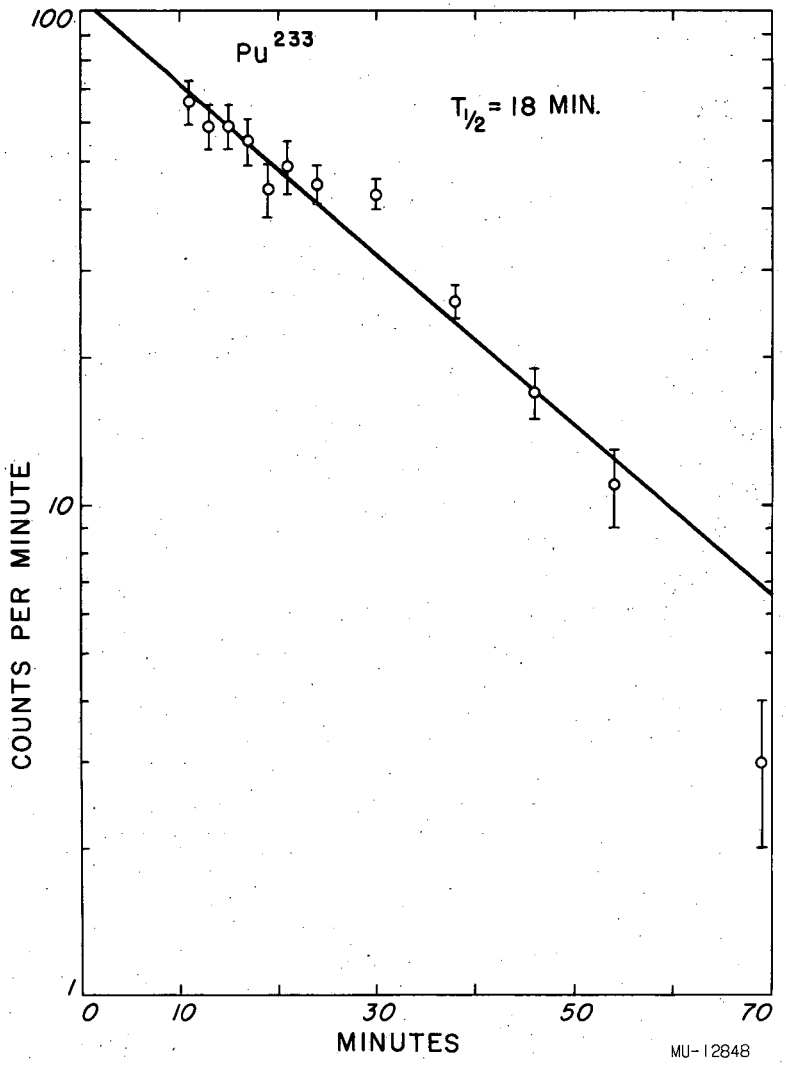

Fig. 14. The decay of Pu^{233}.

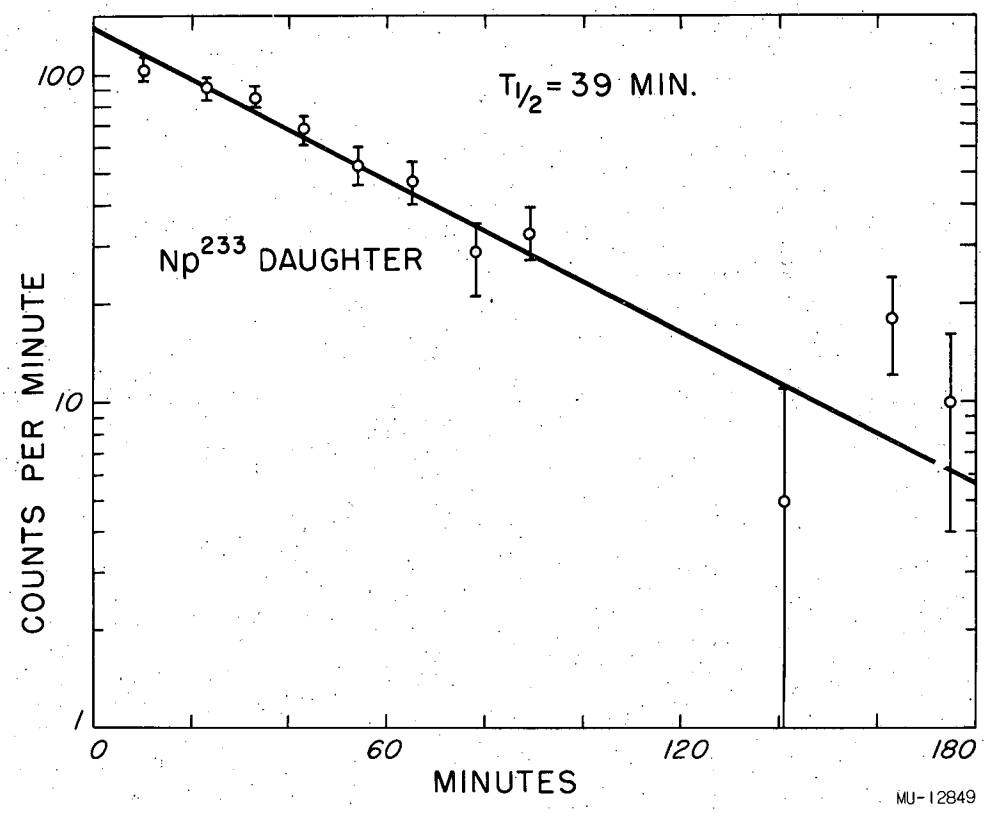

Fig. 15. The decay of Np^{233}.

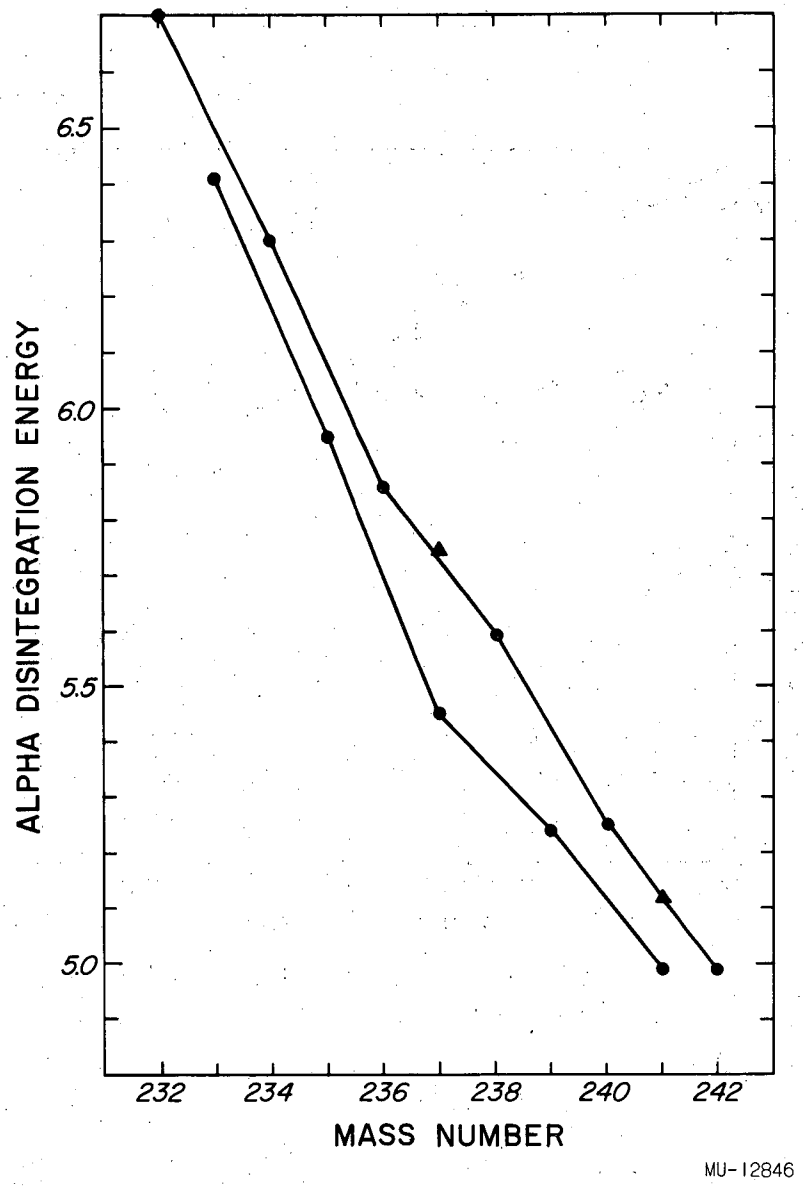

Fig. 16. Alpha-disintegration energy of plutonium isotopes as a function of energy.

ACKNOWLEDGMENTS

I am pleased to acknowledge the guidance and continued interest in this program of Professor Glenn T. Seaborg and Dr. Richard A. Glass.

Bruce M. Foreman, Jr., Walter M. Gibson, Richard M. Lessler, E. Victor Luoma, Robert Vandenbosch, Susanne R. Vandenbosch (nee Ritsema), Paul F. Donovan, and Jose Gonzalez-Vidal have provided technical assistance and stimulating discussions that have been very valuable to me.

I am indebted to Bernard G. Harvey and William H. Wade for their advice, and in particular for helpful suggestions about the discussion section.

I wish to thank George Barton for doing the mass analysis of the U^{233} and Maynard C. Michel for doing the mass analyses of the Np^{235} - Np^{237} mixtures.

I am grateful to Herman P. Robinson and Donald Paxson for running the GADAC calculations.

W. Bart Jones, Peter McWalters, John Wood, the late G. Bernard Rossi, and other members of the crew of the Crocker Laboratory 60-inch cyclotron have been very helpful and co-operative.

The assistance of the Health Chemistry Group under the direction of Nelson Garden is appreciated, especially that of Sue Hargis, Roberta Delk, and Marshall Lombardo.

Thanks are due to Therese Pionteki, who has had the tedious task of doing the Geiger counting of many of my samples.

I am grateful to Patricia Howard for typing the Multilith originals for this thesis.

I wish to thank the National Science Foundation for providing me with three National Science Foundation Predoctoral Fellowships during the course of this work.

This work was performed under the auspices of the U. S. Atomic Energy Commission.

APPENDIX A

COUNTING EFFICIENCIES

Introduction

That the efficiency with which the Nucleometer detects electron-capture events varies from nuclide to nuclide has been a source of difficulty to all who have tried to determine absolute disintegration rates with this instrument. Several experimenters using several different techniques have measured the counting efficiency of this instrument for the electron-capture decay of a number of different nuclides.[21,25,84]

In order to discuss Nucleometer counting efficiencies, it is necessary to define several expressions. "The counting efficiency of (or for) Pu^{235}" is to be understood to mean the ratio of the number of events detected by the Nucleometer to the total number of electron-capture disintegrations of Pu^{235}. The fluorescence yield is the number of x-rays emitted by an atom for every electron vacancy. Hence, the K-fluorescence yield is the number of K x-rays emitted for every vacancy in the K electron shell of the atom. An Auger electron is an electron emitted when a vacancy is filled by an electron from a higher shell without the emission of an x-ray. The energy with which the Auger electron is emitted is equal to the energy difference between the two levels minus the binding energy of the emitted electron. The Auger coefficient is the number of electrons emitted per electron vacancy, and is equal to unity minus the fluorescence yield.

In the electron-capture process, an electron may be captured from any one of the electron shells (provided that the decay energy is greater than the electron binding energy). The daughter atom is left in an excited state, and de-excites either by emission of x-rays or by the Auger process. It is possible to detect electron-capture events either with a detector sensitive to x-rays or with one sensitive to electrons. The Nucleometer is of the latter type.

In the very heavy elements, K fluorescence yields are of the order of 97%[85] and L fluorescence yields 40%.[86] Hence, for 100 K-vacancies, 97 are filled with the emission of K x-rays and 3 with the

emission of Auger electrons. The result is 103 vacancies in the L and higher shells. About 60 electrons are emitted as these vacancies are filled, but these are electrons of energies of the order of 25 kev. By this process, a cascade of low-energy electrons is emitted for each K- or L-shell vacancy. Because the electrons have low energies, the counting efficiency of the detector is very sensitive to sample thickness. The problem is further complicated if the electron capture occurs to an excited state of the daughter nucleus with subsequent emission of conversion electrons.

Methods of Measuring Counting Efficiencies

Three methods have been found particularly useful in determining Nucleometer counting efficiencies: "milking" of alpha-particle-emitting daughters, K x-ray counting, and mass spectrometry.

If a nucleus decaying by electron capture decays to a daughter which is alpha unstable and which has a sufficiently short alpha half life that the alpha activity is intense enough to be detected, it is possible to determine the electron-capture disintegration rate of the parent from the alpha-disintegration rate of the daughter. This method has been used by Gibson[25] to measure the counting efficiency of Np^{234}.

If it is known that the only K-electron vacancies are due to K-electron capture, or if it is possible to correct for the number of K-electron vacancies resulting from the emission of conversion electrons, the K x-ray counting rate may be used to determine the disintegration rate. The number of K x-rays emitted per minute divided by the K-fluorescence yield (0.97 for uranium)[85] gives the number of K vacancies per minute. To calculate disintegrations per minute, it is necessary to make a correction for the number of disintegrations occurring through capture of electrons from the L or higher shells; hence, the ratios of K capture, to M capture, and so forth must be known. In this work, the values that were used for the ratio of K- to L-electron capture either had been measured or were estimated on the basis of the theoretical work of Brysk and Rose.[82] The contribution of capture from the M and higher shells was neglected.

When the nuclide whose counting efficiency is to be determined has a long half life, it is possible to use a third method, mass spectrometry. An example is the procedure used for Np^{235}. A sample containing about 10^{-9} g of Np^{235} was prepared by the (d,2n) reaction on U^{235} and purified by the methods described in Chapter II. To this sample was added a similar amount of Np^{237}, and a portion of the sample was subjected to mass analysis to determine the ratio of the number of atoms of Np^{235} to the number of atoms of Np^{237}. The alpha activity from a second portion of the same sample was analyzed in an alpha-pulse analyzer to determine what fraction of the total alpha activity was due to Np^{237}. The absolute alpha-disintegration rate of the same sample was measured in an ionization chamber of 52% geometry. From the absolute alpha-disintegration rate, the percentage of the alpha activity due to Np^{237}, the half lives of Np^{237} and Np^{235},[47] and the atom ratio of Np^{237} and Np^{235}, it was possible to calculate the absolute disintegration rate of Np^{235} in the sample. When the intensity of the same sample had been measured in the Nucleometer, the counting efficiency was calculated by dividing the measured intensity by the absolute disintegration rate.

Results

The counting efficiency of Np^{235} was determined both by K x-ray counting, using the ratio of L- to K-electron capture of 30 measured by Hoff, Olsen, and Mann,[87] and by the mass-spectrometric method just described. The value determined by the former method was greater than 100%, by the latter, 41%. Using a factor estimated from the work of Brysk and Rose[82] to correct the first number for contributions from capture from the M and higher shells brings the value down to about 90%, leaving a discrepancy of a factor of two to be explained. It is possible that, because of the very low decay energy of Np^{235}, (180 kev)[88] capture from the M and higher shells makes a higher contribution to the total number of disintegrations than would be expected on theoretical grounds. It is also possible that the sample subjected to mass analysis contained U^{235} impurity, with the result that the counting efficiency would appear to be lower than it actually is. However, mass analyses run at different filament temperatures indicated that the amount of U^{235} that may have been present was not sufficient to account for the observed discrepancy.

The various counting efficiencies used in this work are summarized in Table VI.

Table VI

Nucleometer Counting Efficiencies

Nuclide	Counting efficiency	Source
Np^{233}	0.80 ± 0.20	a
Np^{234}	0.63 ± 0.02	b
Np^{235}	0.41 ± 0.04	c
Np^{236}	0.92 ± 0.20	d
Pu^{235}	0.70 ± 0.14	e

a. Estimated.

b. Reference 25, by milking U^{234}.

c. This work, mass spectrometry.

d. Reference 21, milking of Pu^{236}. Electron capture to beta minus ratio measured by T. O. Passell, Internal Conversion of Gamma Radiation in the L Subshells, Ph.D. thesis, University of C lifornia, 1954; also University of California Radiation Laboratory Unclassified Report UCRL-2528 (March, 1954).

e. This work, K x-ray counting using an estimated L/K ratio of 0.23.

An incidental result of the work on counting efficiencies has been the determination of the partial alpha half lives of Np^{235} and Pu^{235} (the latter done in collaboration with Vandenbosch).[a] The value determined for Np^{235} is $(9.1 \pm 0.7) \times 10^4$ years, in disagreement with the value determined by Hoff and co-workers of $(3.2 \pm 0.3) \times 10^4$ years.[87] That for Pu^{235} is 1.7 ± 0.4 years. Because of the discrepancies in the values of the counting efficiency and partial alpha half life of Np^{235}, it would be desirable to remeasure these quantities.

APPENDIX B

AIDS FOR RESOLVING DECAY CURVES

If the half lives are known for the various isotopes whose decay is contributing to a decay curve, certain devices may sometimes be used as aids in resolving the curves.

The simplest of these is the "synthetic plot" mentioned by Shudde.[50] A curve calculated on the basis of the half lives of the nuclides thought to be present is plotted on semilog graph paper of the same scale as that on which the experimental data are plotted. The sheet on which the experimental curve is drawn is placed over that on which the synthetic curve is drawn, and, with corresponding co-ordinate axes kept parallel, the two sheets are moved around until the two curves coincide. The components of the synthetic curve, when traced onto the sheet having the experimental curve, become the components of the experimental curve. This technique is useful when there are two experimental components in the decay curve or when it is necessary to correct for the growth of a long-lived daughter.

The so-salled Biller plot[49] may also be used where there are two components decaying independently. The total activity, A, at time t is given by the formula

$$A = A_1^o e^{-\lambda_1 t} + A_2^o e^{-\lambda_2 t} ,$$

where A_1^o and A_2^o are the initial activities of components 1 and 2, and the λ's are the respective decay constants. Dividing the equation by $e^{-\lambda_2 t}$ gives

$$Ae^{+\lambda_2 t} = A_1^o e^{-t(\lambda_1 - \lambda_2)} + A_2^o .$$

Then, if we plot $Ae^{\lambda_2 t}$ versus $e^{-t(\lambda_1 - \lambda_2)}$, we get a straight line, whose slope is A_1^o and whose intercept is A_2^o. This relationship is particularly useful when the half lives of the two components are close in value.

A plot similar to the Biller plot relating parent and daughter decay has been devised. The total activity of the sample is given by

$$A = (N_1^o \lambda_1 C_1)e^{-\lambda_1 t} + (N_1^o \lambda_1 C_2)\frac{\lambda_2}{\lambda_2 - \lambda_1}(e^{-\lambda_1 t} - e^{-\lambda_2 t}) .$$

A is the total activity at time t, $N_1^o\lambda_1$ is the disintegration rate of the parent at zero time, C_1 and C_2 are the counting efficiencies of parent and daughter respectively, and λ_1 and λ_2 are the decay constants of parent and daughter respectively. Since we have

$$A_1^o = N_1^o \lambda_1 C_1 ,$$

we obtain

$$A = A_1^o e^{-\lambda_1 t} + A_1^o \frac{C_2}{C_1} \frac{\lambda_2}{\lambda_2 - \lambda_1} (e^{-\lambda_1 t} - e^{-\lambda_2 t}) .$$

Dividing the equation by $(e^{-\lambda_1 t} - e^{-\lambda_2 t})$ gives

$$\frac{A}{(e^{-\lambda_1 t} - e^{-\lambda_2 t})} = A_1^o \frac{e^{-\lambda_1 t}}{(e^{-\lambda_1 t} - e^{-\lambda_2 t})} + A_1^o \frac{C_2}{C_1} \frac{\lambda_2}{\lambda_2 - \lambda_1} .$$

Plotting $A/(e^{-\lambda_1 t} - e^{-\lambda_2 t})$ versus $e^{-\lambda_1 t}/(e^{-\lambda_1 t} - e^{-\lambda_e t})$ gives a straight line whose slope is A_1^o and whose intercept is $A_1^o (C_2/C_1) (\lambda_2/(\lambda_2 - \lambda_1))$. This type of plot is particularly useful when λ_2 is only slightly greater than λ_1, with the result that equilibrium is not established. The method was used effectively to resolve the curve representing the decay of the $Zr^{95} - Nb^{95}$ system, where the half lives are 65 and 35 days, respectively.

It is possible to devise other such plots for specialized circumstances. The disadvantages of these methods are that they require the assumption that the decay curve has no other components than those given by the formula, and also require that the half lives be known accurately.

APPENDIX C

CLASSICAL MODEL FOR STRIPPING REACTIONS

It is possible to use a simple classical model to show reasonableness of the idea that when a heavy element is bombarded with helium ions, tritons can be produced in such a manner as to leave the nucleus with a low excitation. We shall consider a helium ion of energy E and impact parameter b, such that the trajectory of the helium ion is tangent to the surface of the nucleus. At the point of contact, the helium ion splits into a triton and a proton, the proton being absorbed by the nucleus and the triton continuing initially along the same path as the helium ion and with the same velocity. Figure 17 shows a schematic diagram of the interaction.

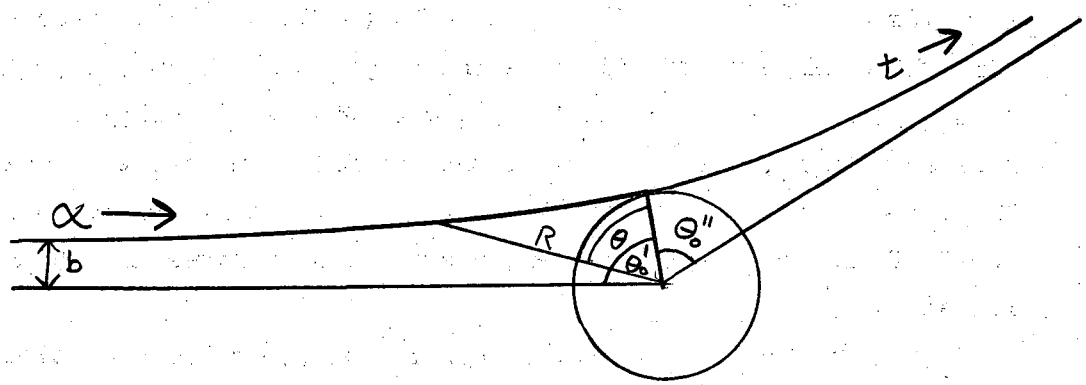

Fig. 17. Schematic diagram of stripping model

If we assume that the nucleus is stationary and that the potential is a Coulomb potential only, the position of the particle is given by the formula

$$R = a/(d \cos \theta - 1),$$

where

$$a = 2b^2/R_o,$$

$$d^2 = 1 + 4b^2/R_o^2,$$

$$R_o = zZe^2/mv_o^2,$$

R_o is the classical distance of closest approach of the projectile, z the charge of the helium ion or triton, Z the atomic number of the target, m the mass of the projectile, and v_o the initial velocity of the projectile. Setting $R_o = \infty$, we find

$$\theta_o = \arccos(1/d).$$

When $\theta = 0$, R will equal R_c, the sum of the radii of the helium ion (1.2 f (f = fermis = 10^{-13} cm)) and of the target (9.3 f if we assume $r = r_o A^{1/3}$ with $r_o = 1.5$ f). Hence,

$$R_c = a/(d - 1).$$

Substituting the expressions given for a and d and solving for b, we find

$$b^2 = R_c (R_c - R_o) .$$

For a 40-Mev helium ion impinging on a U^{238} target, $R_o = 6.62$ f, and, therefore, b = 6.40 f. Using this value for b, we may solve for d and, hence, θ_o', which is 62.5^o. [89]

The potential energy of the helium ion at the point of contact is $2Ze^2/R_c$, or 25.2 Mev, and its kinetic energy is 14.8 Mev. At this point, a proton is stripped from the helium ion and goes into the nucleus with the velocity of the helium ion. The potential and kinetic energies of the remaining triton are 12.8 and 11.1, respectively, and the excitation energy of the nucleus is 12.4 Mev (the loss of potential energy of the projectile) plus 3.7 Mev (the kinetic energy of the proton) minus 14.5 Mev (the Q of the reaction), or 1.6 Mev – a very low excitation.

The kinetic energy of the triton at $R = \infty$ will be 33.9 Mev, and from this value it is possible to calculate the trajectory of the triton. We find that θ_o'' is equal to 68.8^o and, hence, the angle between the direction of the incident helium ion and that of the outgoing triton is about 50^o.

Making the same set of calculations for the (α,He^3) reaction, we find that the ejected He^3 ion must pass through a region of negative kinetic energy, implying that for this reaction to take place there must be barrier penetration. The conclusion is in agreement with the observed cross sections for the (α,He^3) reaction on U^{238}, which are less than 1 millibarn, as compared with the (α,t) cross sections of up to 20 millibarns.[20,23,24]

Two drawbacks to the model are that the angle at which the triton is emitted is too large compared with the angles measured experimentally,[74] and that for helium ions with initial energies below 34 Mev, the nucleus will be left with a negative excitation, although the cross section for this reaction is still appreciable well below this energy.[20]

LIST OF ILLUSTRATIONS

LIST OF TABLES

REFERENCES

1. N. Bohr, Nature 143, 330 (1939).
2. O. Hahn and F. Strassman, Naturwiss 27, 11 (1939).
3. N. Bohr and J. A. Wheeler, Phys. Rev. 56, 426 (1939).
4. J. Frenkel, Phys. Rev. 55, 987 (1939).
5. G. T. Seaborg, Phys. Rev. 85, 157 (1952).
6. Whitehouse and Galbraith, Nature 169, 494 (1952).
7. W. J. Swiatecki, Phys. Rev. 100, 937 (1955).
8. R. Vandenbosch, University of California Radiation Laboratory (unpublished data).
9. A. Turkevich and J. B. Niday, Phys. Rev. 84, 52 (1951); Keller, Steinberg and L. E. Glendenin, Phys. Rev. 94, 969 (1954); E. P. Steinberg and L. E. Glendenin, Phys. Rev. 95, 431 (1954); R. W. Spence and G. P. Ford, Annual Reviews of Nuclear Science (Annual Reviews, Inc., Stanford, California, 1953) 2, 399 (1953).
10. S. Frankel and N. Metropolis, Phys. Rev. 72, 914 (1947).
11. D. L. Hill and J. A. Wheeler, Phys. Rev. 89, 1102 (1953).
12. M. G. Mayer, Phys. Rev. 74, 235 (1948).
13. L. Meitner, Nature 165, 561 (1950); L. Meitner, Arkiv Fysik 4, 383 (1952).
14. D. Curie, Compt. rend. 235, 1286 (1952); ibid. 237, 1401 (1953); D. Curie, J. phys. radium 15, 733 (1954).
15. J. Frenkel, J. Phys. (USSR) 10, 533 (1946).
16. P. Fong, Phys. Rev. 102, 434 (1956).
17. A. Bohr and B. Mottelson, Dan. Mat. Fys. Medd. 27, No. 16 (1953).
18. The ideas in this paragraph are taken from a paper by A. Bohr from the Proceedings of the International Conference on the Peaceful Uses of Atomic Energy (United Nations, New York, 1956), Vol. 2, p. 151, and from lectures given by B. Mottelson and L. Wilets at Berkeley in 1956 and 1957.

19. Glass, Carr, Cobble, and Seaborg, Phys. Rev. 104, 434 (1956).

20. S. E. Ritsema, Fission and Spallation Excitation Functions of U^{238} (M. S. thesis), UCRL-3266, January 1956.

21. R. Vandenbosch, University of California Radiation Laboratory, unpublished data.

22. G. E. Gordon, University of California Radiation Laboratory, unpublished data.

23. P. F. Donovan, University of California Radiation Laboratory, unpublished data.

24. J. A. Coleman, University of California Radiation Laboratory, unpublished data.

25. W. M. Gibson, Fission and Spallation Competition from the Intermediate Nuclei Americium-241 and Neptunium-235 (thesis), UCRL-3493, November 1956.

26. B. M. Foreman, University of California Radiation Laboratory, unpublished data.

27. E. V. Luoma, Deuteron-Induced Spallation and Fission Reactions in Plutonium Isotopes (M. S. thesis) UCRL-3495, November 1956.

28. R. M. Lessler, University of California Radiation Laboratory, unpublished data.

29. Harvey, Chetham-Strode, Ghiorso, Choppin, and Thompson, Phys. Rev. 104, 1315 (1956).

30. For instance, cross sections for the reactions Pb^{208} $(\alpha,2n)$ Po^{210} and Pb^{208} (α,pn) Bi^{210} of 400 mb and 8 mb, respectively, with 40-Mev helium ions are reported by Templeton, Howland, and Perlman, Phys. Rev. 72, 766 (1947); and ibid., page 758.

31. Wade, Gonzalez-Vidal, Glass, and Seaborg, Spallation-Fission Competition in Heaviest Elements; Triton Production, to be published; also UCRL-3640, March 1957.

32. Hyde, Studier, and Ghiorso, The Transuranium Elements: Research Papers Ed. by Seaborg, Katz, and Manning. National Nuclear Energy Series, Plutonium Project Record, (McGraw-Hill, New York, 1949), Vol. 14B, paper 22.15, p. 1622.

33. Perlman, Morgan, and O'Connor, op.cit., paper 22.30, p. 1651; Perlman, Morgan, and O'Connor, AECD-2289, September 1948.

34. Magnusson, Thompson, and Seaborg, Phys. Rev. 78, 363 (1950).

35. D. A. Orth, Isotopes of Neptunium and Plutonium (thesis), UCRL-1059 (Rev.), March 1952. Also unpublished data.

36. Cohen, Farrell-Bryan, Coombes, and Hullings, Phys. Rev. 98 685 (1955).

37. Nelson Garden, University of California Radiation Laboratory, unpublished data.

38. D. S. Hufford and B. F. Scott, The Transuranium Elements: Research Papers Ed. by Seaborg, Katz, and Manning. National Nuclear Energy Series, Plutonium Project Record, (McGraw-Hill, New York, 1949), Vol. 14B, paper 16.1, p. 1149.

39. R. A. Glass, Studies in the Nuclear Chemistry of Plutonium, Americium, and Curium and the Masses of the Heaviest Elements (thesis), UCRL-2560, April 1954.

40. Aron, Hoffman, and Williams, Range-Energy Curves AECU-663, May 1951.

41. Magnusson, Huizenga, Siddall, and Studier, ANL.4667, May 1951.

42. W. Meinke, Chemical Procedures Used in Bombardment Work at Berkeley UCRL-432 and supplements, August 1949.

43. M. Lindner, Radiochemical Procedures in Use at the University of California Radiation Laboratory (Livermore) UCRL-4377, August 1954.

44. F. L. Moore, A Solvent Extraction Method for Neptunium-237 Analysis ORNL-961, July 1951.

45. W. E. Nervik, J. Phys. Chem. 59, 690 (1955).

46. A. Chetham-Strode, Jr., Light Isotopes of Berkelium and Californium (thesis), UCRL-3322, June 1956.

47. Hollander, Perlman, Seaborg, Revs. Modern Phys. 25, 469 (1953).

48. Prestwood, Smith, Browne, and Hoffman, Phys. Rev. 98, 1324 (1955).

49. W. F. Biller, Characteristics of Bismuth Fission Induced by 340-Mev Protons (thesis), UCRL-2067, December 1952.

50. R. Shudde, Fission of Uranium with 5.7-Bev Protons (thesis), UCRL-3419, June 1956.

51. I. Perlman and J. O. Rasmussen, in Handbuch der Physik, 42, (to be published); also UCRL-3424, June 1956.

52. W. E. Nervik and P. C. Stevenson, Nucleonics 10, 18 (1952).

53. H. S. Hicks and R. S. Gilbert, Phys. Rev. 100, 1286 (1955).

54. B. P. Burtt, Nucleonics 8, 28 (1949).

55. B. M. Foreman, Jr. and R. A. Glass, University of California Radiation Laboratory, unpublished.

56. Glendinin, Coryell, and Edwards, Radiochemical Studies: The fission Products (McGraw-Hill Book Company, Inc., New York, 1951), Edited by C. D. Coryell and N. Sugarman, National Nuclear Energy Series, Div. IV, Vol. 9, paper 52; A. Pappas, in Proceedings of the International Conference on the Peaceful Uses of Atomic Energy (United Nations, New York, 1956), Vol. 7, p. 19.

57. R.H. Goeckermann and I. Perlman, Phys. Rev. 73, 1127 (1948).

58. For a table of the average number of neutrons emitted in spontaneous and slow-neutron-induced fission of very heavy elements, see E. K. Hyde and G. T. Seaborg, Handbuch der Physik, 39, (to be published); UCRL-3312, February 1956.

59. R. A. Glass, University of California Radiation Laboratory, unpublished data.

60. J. M. Blatt and V. F. Weisskopf, Theoretical Nuclear Physics, (Wiley, New York, 1952).

61. E. K. Hyde, The Transuranium Elements: Research Papers Ed. by Seaborg, Katz, and Manning. National Nuclear Energy Series, Plutonium Project Record, (McGraw-Hill, New York, 1949), Vol. 14B, paper 19.15, p. 1431.

62. E. Potter, University of California Radiation Laboratory, private communication.

63. W. B. Jones and P. McWalters, University of California Crocker Laboratory, private communication.

64. Peter Fong, private communication via John Alexander.

65. R. J. Carr, Spallation-Fission Competition in the Nuclear Reactions of Plutonium Induced by Alpha Particles (thesis), UCRL-3395, April 1956.

66. J. D. Jackson, Fission by Mev Neutrons, in Proceedings of the Symposium on the Physics of Fission Held at Chalk River, Ontario, May 14-18, 1956. Ed. by Hanna, Milton, Sharp, Stevens, and Taylor, CRP-642-A, p. 125.

67. See also J. R. Huizenga and R. B. Duffield, Phys. Rev. 88, 959 (1952).

68. J. D. Jackson, Can. J. Phys. 34, 767 (1956).

69. McManus, Sharp, and Gellmann, Phys. Rev. 93, 924A (1954); McManus, and Sharp, unpublished data.

70. R. Serber, Phys. Rev. 72, 1114 (1947).

71. S. T. Butler, Proc. Roy. Soc. (London) A208, 559 (1951).

72. S. T. Butler, Phys. Rev. 106, 272 (1957).

73. E. L. Kelly, Excitation Functions of Bismuth (thesis) UCRL-1044, December 1950.

74. W. H. Wade and J. Gonzalez-Vidal, University of California Radiation Laboratory, unpublished data.

75. Amiel, Harvey, and Wade, University of California Radiation Laboratory, unpublished data.

76. Much of the material discussed in this section has also been presented by Thomas, Vandenbosch, Glass, and Seaborg, Phys. Rev. 106, 1228 (1957).

77. H. P. Robinson and G. O. Brink, GADAC, in Chemistry Division Quarterly Report, UCRL-2355, p. 14, September 1953.

78. The energy thresholds for the various reactions are calculated from the atomic masses by Glass, Thompson, and Seaborg, J. Inorg. Nucl. Chem. 1, 3 (1954).

79. See Appendix A for a discussion of counting efficiencies.

80. Perlman, Ghiorso, and Seaborg, Phys. Rev. 77, 26 (1950).

81. R. W. Hoff and S. G. Thompson, Phys. Rev. 96, 1350 (1954).

82. H. Brysk and M. E. Rose, ORNL-1830, 1955.

83. R. W. Hoff and J. O. Rasmussen, Phys. Rev. 101, 280 (1956).

84. E. K. Hulet, An Investigation of the Isotopes of Berkelium and Californium (thesis), UCRL-2283, July 1953.

85. P. R. Gray, Phys. Rev. 101, 1306 (1956).

86. B. B, Kinsey, Can. J. Research A26, 404 (1948).

87. Hoff, Olsen, and Mann, Phys. Rev. 102, 805 (1956).

88. Calculated by the method of closed cycles. See Reference C.

89. D. Halliday, Introductory Nuclear Physics (Wiley, New York, 1950), p. 300.